

Accepted Manuscript

Optimization of a 1,3,4-oxadiazole series for inhibition of Ca^{2+} /calmodulin-stimulated activity of adenylyl cyclases 1 and 8 for the treatment of chronic pain

Jatinder Kaur, Monica Soto-Velasquez, Zhong Ding, Ahmadreza Ghanbarpour, Markus A. Lill, Richard M. van Rijn, Val J. Watts, Daniel P. Flaherty

PII: S0223-5234(18)30995-4

DOI: <https://doi.org/10.1016/j.ejmech.2018.11.036>

Reference: EJMECH 10893

To appear in: *European Journal of Medicinal Chemistry*

Received Date: 21 August 2018

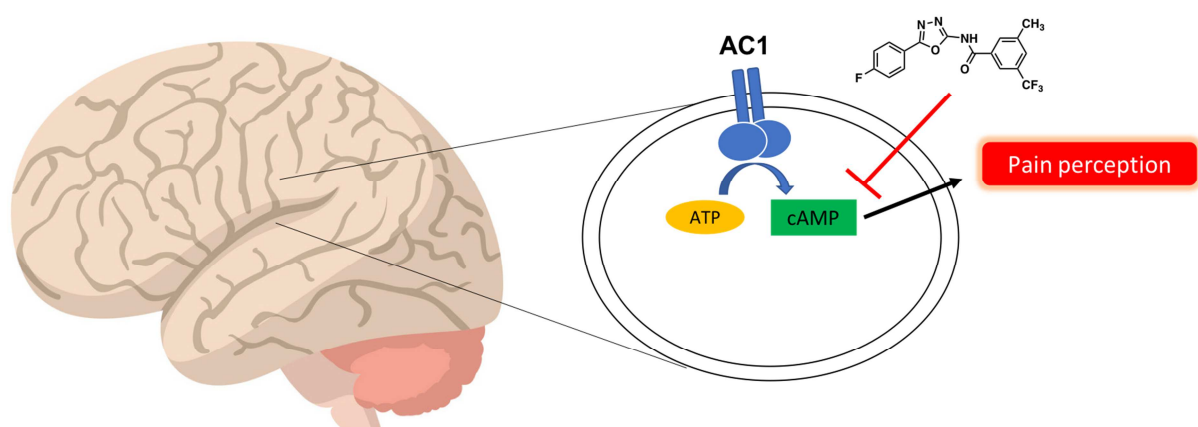
Revised Date: 12 November 2018

Accepted Date: 15 November 2018



Please cite this article as: J. Kaur, M. Soto-Velasquez, Z. Ding, A. Ghanbarpour, M.A. Lill, R.M. van Rijn, V.J. Watts, D.P. Flaherty, Optimization of a 1,3,4-oxadiazole series for inhibition of Ca^{2+} /calmodulin-stimulated activity of adenylyl cyclases 1 and 8 for the treatment of chronic pain, *European Journal of Medicinal Chemistry* (2018), doi: <https://doi.org/10.1016/j.ejmech.2018.11.036>.

This is a PDF file of an unedited manuscript that has been accepted for publication. As a service to our customers we are providing this early version of the manuscript. The manuscript will undergo copyediting, typesetting, and review of the resulting proof before it is published in its final form. Please note that during the production process errors may be discovered which could affect the content, and all legal disclaimers that apply to the journal pertain.



Optimization of a 1,3,4-oxadiazole series for inhibition of Ca^{2+} /calmodulin-stimulated activity of adenylyl cyclases 1 and 8 for the treatment of chronic pain

Jatinder Kaur^a, Monica Soto-Velasquez^a, Zhong Ding^a, Ahmadreza Ghanbarpour^a, Markus A. Lill^{a,b,c}, Richard M. van Rijn^{a,b,c}, Val J. Watts^{a,b,c}, and Daniel P. Flaherty^{a,b,c,*}

^a Department of Medicinal Chemistry and Molecular Pharmacology, College of Pharmacy, Purdue University, 575 Stadium Mall Dr., West Lafayette, IN 47907.

^b Purdue Institute for Drug Discovery, Purdue University, West Lafayette, IN 47907

^c Purdue Institute for Integrative Neuroscience, Purdue University, West Lafayette, IN 47907

* Corresponding author E-mail address: dflaher@purdue.edu (D.P. Flaherty)

Keywords

Adenylyl cyclase inhibitors; 1,3,4-oxadiazole; Chronic pain treatment, Molecular modeling

Abstract

Adenylyl cyclases type 1 (AC1) and 8 (AC8) are group 1 transmembrane adenylyl cyclases (AC) that are stimulated by Ca^{2+} /calmodulin. Studies have shown that mice depleted of AC1 have attenuated inflammatory pain response, while AC1/AC8 double-knockout mice display both attenuated pain response and opioid dependence. Thus, AC1 has emerged as a promising new target for treating chronic pain and opioid abuse. We discovered that the 1,3,4-oxadiazole scaffold inhibits Ca^{2+} /calmodulin-stimulated cyclic adenosine 3',5'-monophosphate (cAMP) production in cells stably expressing either AC1 or AC8. We then carried out structure-activity relationship studies, in which we designed and synthesized 65 analogs, to modulate potency and selectivity versus each AC isoform in cells. Furthermore, molecular docking of the analogs into an AC1 homology model suggests the molecules may bind at the ATP binding site. Finally, a prioritized analog was tested in a mouse model of inflammatory pain and exhibited modest analgesic properties. In summary, our data indicate the 1,3,4-oxadiazoles represent a novel scaffold for the cellular inhibition of Ca^{2+} /calmodulin-stimulated AC1- and AC8 cAMP and warrant further exploration as potential lead compounds for the treatment of chronic inflammatory pain.

1. Introduction

Adenylyl cyclases (ACs) are key effectors of G protein-coupled receptor (GPCR) signaling pathways that catalyze the production of the secondary messenger molecule cyclic adenosine 3',5'-monophosphate (cAMP) from adenosine triphosphate (ATP) [1]. Many cellular responses are mediated by changes in intracellular cAMP, and ACs play crucial roles in various physiological processes including learning, memory, chronic pain, and drug abuse [2, 3]. ACs serve as downstream effectors for various GPCRs including the μ -opioid receptor (μ OR), the preferred target for analgesic drugs [4]. Agonism of the μ OR induces dissociation of the inhibitory G-protein α_i ($G\alpha_i$) subunit from the heterotrimeric G-protein complex, which then inhibits AC activity and reduces cAMP levels and propagating the desired analgesic effect [5]. Subsequently, μ OR activation also leads to the recruitment of β -arrestins, which mediate the undesired side-effects such as tolerance, respiratory depression and constipation commonly associated with opioid pain management [4, 6-8]. Thus, there is ongoing research to design biased modulators of the μ OR with the aim of increasing the desired analgesic properties via the G-protein, while simultaneously reducing the unwanted side-effects induced by β -arrestin signaling [9]; however, this has been notoriously difficult to achieve. Alternatively, we [10], and others [11], have proposed inhibiting the activity of the downstream ACs – effectively bypassing the μ OR – may represent a promising strategy for the development of drugs to treat chronic pain while limiting the undesired side-effects associated with opioid treatment.

There are nine membrane-bound AC isoforms categorized into four distinct groups [12]. All ACs are activated by the stimulatory $G\alpha_s$ protein and can also be regulated by alternative mechanisms including $G\beta\gamma$ subunits, calmodulin, protein kinases and cations, but these regulatory mechanisms differ between the four distinct groups. Group 1 ACs include AC1, AC3, and AC8 and are characterized by regulation with Ca^{2+} /calmodulin; group 2 ACs comprising AC2, AC4, and AC7 are conditionally activated by $G\beta\gamma$ subunits; group 3 ACs consisting of AC5 and AC6 and are inhibited by Ca^{2+} ; and the Group 4 AC, AC9, is the only AC insensitive to forskolin activation. Although cells typically express multiple AC isoforms, specific tissue expression patterns coupled with distinct regulatory properties of the AC isoforms have led to certain isoforms being implicated with particular pathophysiology [12]. For example, AC1 and AC8 are highly expressed in the brain, within the hippocampus (associated with learning and memory) [13, 14] and the anterior cingulate cortex

(ACC, associated with chronic pain perception) [2, 15]. Additionally, AC1 knockout (AC1^{-/-}) and AC1/AC8 double knockout (DKO) mice have exhibited reduced or abolished behavioral responses to two inflammatory pain stimuli (formalin and complete Freund's adjuvant, CFA) [16, 17]. Even though, the DKO mice also exhibited behaviors consistent with severe memory impairment, these memory deficits were attenuated or not observed in the AC1 knockout mice [18]. Hence, these results and the distinct tissue specific expression of AC1 in pain perception regions of the ACC, suggests AC1 represents an attractive target for therapeutic development of pain management treatments.

The current state-of-the-art for AC1 inhibitors (**Fig. 1**) includes adenosine-based inhibitors represented by SQ22536 [19] that are proposed to bind in a non-competitive way at the catalytic site "P"-site. This class typically only exhibits modest (> 10 μ M) AC potency in cellular assays, and non-selectively inhibit the catalytic activity of AC isoforms [20]. This weak activity was confirmed with our data for SQ22536 against HEK-AC1 cells stimulated by forskolin (**Fig. S1**). More recently, pharmacological data from the molecule NB001 supported genetic evidence that implicated AC1s role in pain

perception by attenuating chronic pain response (inflammatory and neuropathic) in both mice and rats treated with the molecule [21, 22]. However, while effective in *in vivo* models for chronic pain, NB001 has moderate activity against AC1 (IC_{50} = 10 μ M) in the cell-based Ca^{2+} /calmodulin-mediated cAMP accumulation assay [22]. Furthermore, while it is hypothesized to bind at the P-site recent data suggests that it does not directly inhibit AC1 but rather it acts through an alternative mechanism [23]. Additionally, due to the adenosine-like structures of NB001 and SQ22536 concerns have been raised that adenosine-based molecules could interfere with other cellular processes such as DNA synthesis [19, 20, 23] limiting the advancement of P-site inhibitors for further development. Finally, our team has previously reported a chromone-based inhibitor, ST034307, with single-digit micromolar potency versus AC1 (cellular IC_{50} value of 2.3 μ M), no inhibition versus AC8, and efficacy against allodynia in a phenotypic mouse model of inflammatory pain [24]. Unfortunately, the potency of the chromone-based molecule was not able to be further optimized through medicinal chemistry efforts (unpublished results). Additionally, the trichloromethyl moiety can act as an electrophilic center leading to

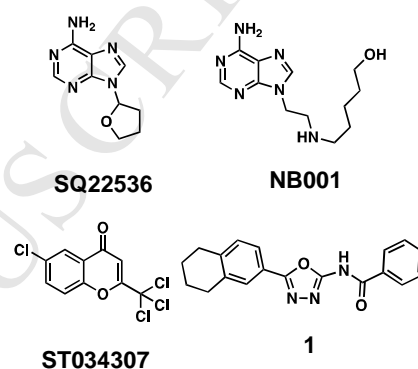


Figure 1. Representative structures of the current state of AC1 inhibitors. Molecule **1** discovered in our screening campaign and the basis for the structure-activity relationship optimization described.

undesired toxicity via non-specific covalent modification of off-target proteins. Attempts to remove this functionality led to complete loss of activity versus AC1 and, therefore, the scaffold was not pursued further. These representative AC1 inhibitors is not an exhaustive list and have significant drawbacks, however, the preliminary *in vivo* data suggest AC1 is a viable target for the treatment of chronic pain. Therefore, our team has embarked upon an AC1 inhibitor discovery program.

To this end, we carried out a phenotypic cell-based high-throughput screen in human embryonic kidney (HEK) cells stably expressing AC1 to identify small molecules with the ability to reduce AC1-mediated production of cAMP upon stimulation with the Ca^{2+} ionophore, A23187 (manuscript in preparation to describe the screen and results). This screen identified the 1,3,4-oxadiazole containing molecules, represented by hit **1**, as a promising scaffold that reduced cAMP levels in cells stably expressing AC1 upon stimulation with Ca^{2+} /calmodulin by more than 90% at a single dose of 10 μM compared to DMSO-treated controls. Hit compound **1** was synthesized by our team (described below) and validated as an inhibitor of AC1-mediated cAMP production with a cellular IC_{50} value of $3.4 \pm 1.0 \mu\text{M}$ in AC1 expressing cells. This molecule was also observed to inhibit AC8 activity with an IC_{50} of $19 \pm 5 \mu\text{M}$ and displayed approximately 5.5-fold selectivity for AC1 over AC8 and data from the resynthesized molecule was comparable to the commercially available dry powder. Our team then designed and synthesized novel analogs for this 1,3,4-oxadiazole series with the aim to improve potency and/or selectivity in the HEK-AC1 and AC8 cell models. A prioritized analog was selected to test for *in vivo* efficacy in an inflammatory pain model. The results of these studies are presented below.

2. Results

2.1. Structure-activity relationship (SAR) strategy

The 1,3,4-oxadiazole series emerged as a hit scaffold from a cell-based cAMP accumulation assay in HEK cells stably expressing AC1. The screen identified 41 hits that contained the 1,3,4-oxadiazole core and displayed more than 90% inhibition of Ca^{2+} /calmodulin-stimulation of AC1 activity when tested at a single dose of 10 μM compared to DMSO

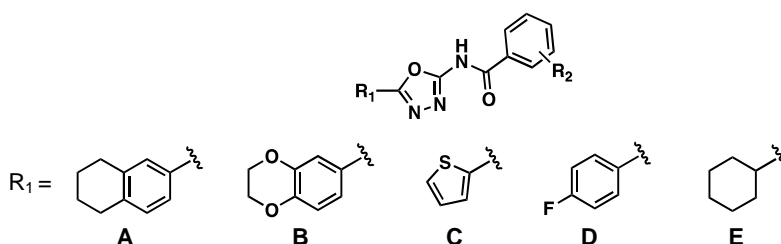


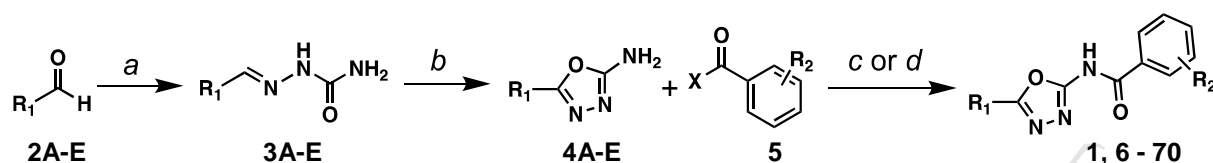
Figure 2. R₁ functional groups prioritized to be part of SAR optimization design strategy of the 1,3,4-oxadiazole scaffold.

controls. The scaffold was not flagged in cheminformatics filters that identify problematic PAINS [25, 26] or aggregators [27]. Therefore, dry powders were reordered of twelve hit compounds, and dose-response curves were generated to determine the potency and maximal efficacy of the compounds against both AC1 and AC8 (IC₅₀ values for the reordered dry powders reported in Supplementary **Table S1**). All re-tested hit compounds inhibited Ca²⁺/calmodulin-mediated cAMP production in both AC1 and AC8 containing cells in a dose-dependent manner, with IC₅₀ values ranging from 2 μ M to 10 μ M against AC1 and 5 μ M to 21 μ M against AC8. The goals of the SAR optimization campaign were then prioritized in the following order: 1) improve potency toward AC1-mediated cAMP production, 2) improve selectivity over AC8-mediated cAMP production, 3) maintain low cellular toxicity, and 4) improve physicochemical properties. Due to convenience of synthesis and diversification of R₂ substituents at the final synthetic step (**Scheme 1**), our medicinal chemistry approach focused on only five R₁ group substituents identified in the original hit set with varying levels of cellular potency against AC1 and/or selectivity over AC8 (**Figure 2**). Initial rounds of SAR combined common R₂ substituents with the prioritized R₁ moieties to create nearest-neighbor analogs for comparison of activity data. Then SAR was continued with further diversification to R₂ and cellular AC1 and AC8 cAMP accumulation data was used to assess analogs for further iterative design cycles. In total 65 novel analogs were designed and synthesized using the protocol described below.

2.2. Chemistry

All 1,3,4-oxadiazole derivatives were synthesized using the same 3-step condensation and amide bond formation protocol (**Scheme 1**). First, either substituted aryl or cycloalkyl aldehydes (**2**) were reacted with semicarbazide hydrochloride salt and sodium acetate in methanol/water solution (1:1) at room temperature (RT) for up to 60 minutes at which point a white precipitate was formed to create a suspension. This precipitate was filtered out by vacuum filtration to produce the desired hydrazine carboxamide intermediate (**3**) typically as a white solid and in good yield. Intermediate **3** was subjected to halogen-mediated oxidative cyclization adapted from a published protocol [28] using bromine and sodium acetate in acetic acid while heating to 60 °C for 2 hours to produce the desired 2-amino-1,3,4-oxadiazole intermediate **4** in good yields. Intermediate **4** was then used as the nucleophile in an amide bond formation reaction with various substituted benzoic acids or acyl chlorides (**5**) to form the final products represented by **6 - 70**. All analogs were fully characterized for identity by proton and carbon NMR and mass spectrometry. All analogs were analyzed for purity using high-

performance liquid chromatography (HPLC) and were required to meet or exceed 95% purity before any biological testing of the molecules.



Scheme 1. Representative synthetic protocol for 1,3,4-oxadiazole analogs Reagents and conditions: a) semicarbazide HCl (1.0 eq), sodium acetate (2.0 eq), MeOH:water (1:1), RT, 30 – 60 min, 86 – 98%; b) Br₂ (1.1 eq), sodium acetate (2.0 eq), acetic acid, 60 °C, 2 hr, 70 – 95%; c) if X = OH: oxalyl chloride (1.1 eq), DMF (1 drop), DCM, 0 °C – rt, 1 hr, crude product carried into next step; d) if X = Cl; pyridine, rt, 16 – 24 hr, 2 – 77%. R₁ (A-E) groups depicted in Figure 2.

2.3. AC1 and AC8 activity

The ability to inhibit Ca²⁺/calmodulin-stimulated production of cAMP mediated by both AC1 and AC8 was evaluated for all analogs by measuring cAMP accumulation in HEK cells stably expressing each respective AC. Dose-response curves were generated for each analog starting at 30 μM concentration, and IC₅₀ values were calculated for molecules that showed > 50% inhibition at the 30 μM dose. All the other analogs that exhibited < 50% inhibition in the respective cell lines were labeled with IC₅₀ values as not determined (ND) in data tables with the observed % inhibition at 30 μM reported in parentheses.

Table 1. SAR data for A-series

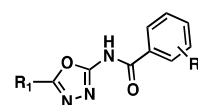
Compd	R ₁ ^a	R ₂	AC1 IC ₅₀ ^{b,c}	AC8 IC ₅₀ ^{b,c}	Fold selectivity ^d
1	A	H	3.4 ± 1.0	19 ± 5	5.6
6	A	3-CF ₃	1.6 ± 0.2	7.9 ± 3.0	4.9
7	A	4-Br	12 ± 3	27 ± 0.2	2.23
8	A	4-OCH(CH ₃) ₂	10 ± 7	12 ± 6	1.2
9	A	3-SCH ₃	1.7 ± 0.7	9.4 ± 2.0	5.5
10	A	3-OCH ₃	3.1 ± 0.4	25 ± 4	8.1
11	A	4-CH ₃	3.4 ± 1.0	25 ± 6	7.4
12	A	4-OCH ₃	6.4 ± 1.0	ND (34%)	> 4.7
13	A	4-F	5.9 ± 1.0	22 ± 4	3.7
14	A	3-F	1.0 ± 0.3	4.2 ± 0.2	4.2
15	A	4-Cl	1.5 ± 1.0	3.6 ± 0.4	2.4
16	A	4-CH ₂ CH ₃	1.2 ± 0.2	2.0 ± 0.4	1.7

^a R₁ modifications corresponding to each letter shown in Fig. 2. ^b IC₅₀ values (μM) represent the mean and SEM for three independent experiments. ^c If analog exhibits > 50% inhibition at 30 μM concentration, the IC₅₀ value was reported. If molecules exhibit < 50% inhibition then the data is listed as not determined (ND) with the percentage inhibition shown in parentheses, ND (XX%). ^d Fold selectivity = AC8 IC₅₀ / AC1 IC₅₀. If the AC8 IC₅₀ value of the compound is ND, then 30 μM used for the AC8 IC₅₀ value to calculate the fold selectivity that is shown with a > symbol.

Beginning with hit **1** our design strategy was to maintain the 5,6,7,8-tetrahydronaphthalene R₁ substituent (A-series) while modifying the phenyl functional group at R₂. Most modifications made to the R₂ component resulted in low-to-mid single digit micromolar potencies (**Table 1**) with selectivity over AC8 ranging

from 1.2 – 8.1-fold. In particular, the 3-CF₃ (**6**, AC1 IC₅₀ = 1.6 ± 0.2 μM), 3-SCH₃ (**9**, 1.7 ± 0.7 μM), 3-F (**14**, 1.0 ± 0.3 μM), 4-Cl (**15**, 1.5 ± 1.0 μM), and 4-CH₂CH₃ (**16**, 1.2 ± 0.2 μM) were slightly more potent against AC1-mediated cAMP production compared to **1** (3.4 ± 1.0 μM). The 3-substituted analogs (**6**, **9**, and **14**) displayed moderate selectivity over AC8, with values of 4.9, 5.5, and 4.2, respectively. However, selectivity was reduced by at least half in the 4-substituted analogs to 2.4 for the 4-Cl (**15**) and 1.7 for the 4-CH₂CH₃ (**16**) analogs. Compared to the hit, analogs **10** and **11** were equipotent versus AC1 (IC₅₀s = 3.1 ± 0.4 μM, and 3.4 ± 1.0 μM) and more selective over AC8 (8.1 and 7.4-fold selectivity, respectively). Rounding out the SAR for the A-series are four 4-position modifications that displayed at least 3.5-fold reduced activity against AC1-mediated cAMP production and reduced selectivity over AC8 compared to the hit. Two pairs of analogs in this series illustrate the apparent preference for 3-substituted over 4-substituted derivatives. The pair represented by **10** and **12** (3-OCH₃ and 4-OCH₃) displayed preference for the meta over para position in AC1 potency. Selectivity was more difficult to assess given that for **12** the IC₅₀ value against AC8 activity was not determined; however, when using % inhibition as a guideline, the selectivity is within the same value as **10**. The second pair represented by analogs **14** and **13** (3-F and 4-F) also clearly indicated a preference for the 3-position substitution in AC1 potency (3-F was 5.9 times more potent than 4-F) with slightly improved selectivity over AC8. Based on the A-series analogs it appears that R₂ modifications at the meta-position were generally beneficial for either AC1 potency and/or selectivity over AC8.

Table 2. SAR data for B- and C-series



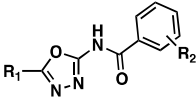
Compd	R ₁ ^a	R ₂	AC1 IC ₅₀ ^{b,c}	AC8 IC ₅₀ ^{b,c}	Fold selectivity ^d
17	B	H	31 ± 3	ND (24%)	>1
18	B	3-SCH ₃	9.5 ± 1.0	ND (37%)	> 3.2
19	B	3-CF ₃	5.1 ± 0.7	32 ± 12	6.3
20	B	4-OCH(CH ₃) ₂	7.5 ± 0.7	ND (39%)	> 4
21	B	4-Br	3.4 ± 0.6	23 ± 2	6.8
22	B	3-OCH ₃	9.6 ± 3.0	ND (18%)	> 3.1
23	B	4-CH ₃	12 ± 4	ND (25%)	> 2.5
24	B	3,4-di-CH ₃	5.3 ± 0.4	14 ± 13	2.6
25	C	H	28 ± 3	ND (18%)	> 1.1
26	C	4-Br	7.7 ± 1.0	ND (41%)	> 3.9
27	C	3-SCH ₃	11 ± 2	ND (34%)	> 2.7
28	C	4-OCH(CH ₃) ₂	11 ± 2	ND (35%)	> 2.7
29	C	4-OCH ₃	15 ± 2	ND (10%)	> 2

^a R₁ modifications corresponding to each letter shown in Fig. 2. ^b IC₅₀ values (μM) represent the mean and SEM for three independent experiments. ^c If analog exhibits > 50% inhibition at 30 μM concentration, the IC₅₀ value was reported. If molecules exhibit < 50% inhibition then the data is listed as not determined (ND) with the percentage inhibition shown in parentheses, ND (XX%). ^d Fold selectivity = AC8 IC₅₀ / AC1 IC₅₀. If the AC8 IC₅₀ value of the compound is ND, then 30 μM used for the AC8 IC₅₀ value to calculate the fold selectivity that is shown with a > symbol.

B-series analogs maintained the 2,3-dihydro-1,4-dioxin-6-yl moiety as the R_1 while altering the R_2 (Table 2). In total only eight analogs were synthesized containing a subset of the same R_2 modifications utilized in the A-series. When comparing nearest neighbor analogs between the A- and the B-series the 5,6,7,8-tetrahydronaphthalene generally outperformed the 2,3-dihydro-1,4-dioxin-6-yl substituent versus AC1 with the exceptions of the 4-Br (**21** compared to **7**) and the 4-OCH(CH₃)₂ (**20** compared to **8**), in which the B-series derivatives were slightly more potent against AC1 activity. The H, 3-CF₃, 3-SCH₃, 3-OCH₃, and 4-CH₃ at the R_2 position in the B-series were less potent than their A-series counterparts. The B-series analogs, however, displayed reduced potency against AC8-mediated cAMP production, but it is difficult to conclude if this reduction arose from a gain in selectivity or just the overall reduced AC potency in general.

C-series analogs containing a 2-thiophene at the R_1 position (Table 2) also proved to be inferior to the A-series analogs. Five analogs were synthesized and tested, and all displayed modest activity on both AC1 and AC8. Therefore, this series was deprioritized from further SAR optimization.

Table 3. SAR data for D-series



Compd	R_1^a	R_2	AC1 IC ₅₀ ^{b,c}	AC8 IC ₅₀ ^{b,c}	Fold selectivity ^d
30	D	H	29 ± 10	ND (8%)	> 1
31	D	4-Br	10 ± 1	ND (33%)	> 3
32	D	3-CF ₃	5.0 ± 0.8	29 ± 1	5.8
33	D	4-CH ₃	7.3 ± 2.0	ND (31%)	> 3.6
34	D	3,4-di-CH ₃	6.5 ± 1.0	ND (42%)	> 4.6
35	D	3-OCH ₃	15 ± 4	ND (23%)	> 2
36	D	4-OCH ₃	13 ± 3	ND (20%)	> 2.3
37	D	3-SO ₂ -piperidine	16 ± 4	ND (38%)	> 1.9
38	D	3-F	11 ± 3	ND (35%)	> 2.7
39	D	4-F	17 ± 2	ND (14%)	> 1.8
40	D	2-F	ND (12%)	ND (13%)	-
41	D	4-CH ₂ CH ₃	8.2 ± 2.0	ND (32%)	> 3.6
42	D	4-Cl	8.9 ± 1.0	ND (11%)	> 3.4
43	D	4-phenyl	2.8 ± 0.6	7.5 ± 1.0	2.7
44	D	3-phenyl	2.3 ± 0.4	7.0 ± 1.0	3.0

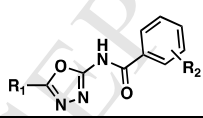
^a R_1 modifications corresponding to each letter shown in Fig. 2. ^b IC₅₀ values (μM) represent the mean and SEM for three independent experiments. ^c If analog exhibits > 50% inhibition at 30 μM concentration, the IC₅₀ value was reported. If molecules exhibit < 50% inhibition then the data is listed as not determined (ND) with the percentage inhibition shown in parentheses, ND (XX%). ^d Fold selectivity = AC8 IC₅₀ / AC1 IC₅₀. If the AC8 IC₅₀ value of the compound is ND, then 30 μM used for the AC8 IC₅₀ value to calculate the fold selectivity that is shown with a > symbol.

The D-series consists of 15 analogs carrying a 4-F-phenyl substituent at the R_1 position (Table 3). In general, the D-series analogs still underperformed compared to their A-series counterparts. There were three

new R₂ functional groups introduced into these analogs that were not tested in the A-series. Analog **40** contained the first ortho-substitution (2-F) of all the series discussed, and it displayed a significant decrease in potency against AC1 activity. Additionally, 4-phenyl (**43**) and 3-phenyl (**44**) derivative performed the best in the D-series (AC1 IC₅₀ values of 2.8 ± 0.6 μM and 2.3 ± 0.4 μM, respectively). However, while these molecules exhibited the best potency toward AC1 it was coupled by a reduction in selectivity over AC8.

Finally, 13 analogs make up the E-series molecules containing a cyclohexyl functional group at the R₁ position (**Table 4**). The change from aromatic to cycloalkyl functionality provided molecules that were generally equipotent to the B-, C-, and D-series and still lagged behind the A-series. However, the E-series appeared to outperform other series when comparing the AC8 potencies. Four analogs from this series (**45**, **51**, **52**, and **54**) displayed single-digit % inhibition values against AC8 when tested at 30 μM, compared to only one such analog in the previous four series (**30**). Additionally, direct comparison of the IC₅₀ values of the 3-F containing analogs (**14**, **38**, and **55**), indicates the E-series was the least potent against AC8 activity. This trend did not correlate with overall AC1 potency as analogs **38** and **55** were equipotent against this isoform but **55** was significantly less potent against AC8. This overall trend is also observed when comparing analogs containing 4-OCH₃ and 4-CH₃ at the R₂ position. However, this trend does not hold when comparing the AC8 potency amongst the 3-SCH₃ analogs. Notably, the 3-phenyl derivative was the most potent E-series molecule against both AC1 and AC8 (IC₅₀s = 1.4 ± 0.2 and 1.4 ± 0.4 μM, respectively).

Table 4. SAR data for E-series



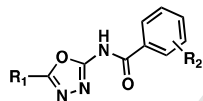
Compd	R ₁ ^a	R ₂	AC1 IC ₅₀ ^{b,c}	AC8 IC ₅₀ ^{b,c}	Fold selectivity ^d
45	E	H	25 ± 2	ND (2%)	> 1.2
46	E	4-Br	8.6 ± 3.0	25 ± 8	2.9
47	E	3-SCH ₃	6.6 ± 3.0	ND (43%)	> 4.5
48	E	3-CF ₃	6.0 ± 0.6	33 ± 7	> 3.6
49	E	3,4-di-CH ₃	8.1 ± 2.0	44 ± 6	5.4
50	E	4-OCH(CH ₃) ₂	10 ± 1	ND (35%)	> 3
51	E	4-OCH ₃	22 ± 3	ND (6%)	> 1.4
52	E	4-CH ₃	16 ± 2	ND (1%)	> 1.9
53	E	4-CH ₂ CH ₃	7.3 ± 3.0	ND (44%)	> 4.1
54	E	4-F	13 ± 1	ND (7%)	> 2.3
55	E	3-F	11 ± 2	ND (11%)	> 2.7
56	E	4-Cl	14 ± 2	ND (10%)	> 2.1
57	E	3-phenyl	1.4 ± 0.2	1.4 ± 0.3	1

^a R₁ modifications corresponding to each letter shown in Fig. 2. ^b IC₅₀ values (μM) represent the mean and SEM for three independent experiments. ^c If analog exhibits > 50% inhibition at 30 μM concentration, the IC₅₀ value was reported. If molecules exhibit < 50% inhibition then the data is listed as not determined (ND) with the percentage inhibition shown in parentheses, ND (XX%). ^d Fold selectivity = AC8 IC₅₀ / AC1 IC₅₀. If the AC8 IC₅₀ value of the compound is ND, then 30 μM used for the AC8 IC₅₀ value to calculate the fold selectivity that is shown with a > symbol.

After design and synthesis of 57 analogs our team chose three R₁ substituents (A, D, and E) to pair with combined modifications to the R₂ side of the molecule (**Table 5**) in an attempt to merge AC1 potency driving functional groups with AC8 selectivity driving functional groups (**58 – 66**). We chose to incorporate a meta-substituted CF₃ in all combined R₂ side modifications as this functional group was consistently among the top potent molecules for each series. We then paired the CF₃ with one other modification either meta-substituted methyl or methoxy or para-substituted methyl. These functional groups were chosen because they consistently provided reduced AC8 potency. The resulting analogs displayed no improvement to AC1 potency or selectivity over AC8. However, one molecule (**61**) containing the 4-fluorophenyl R₁ coupled with 3-CH₃-5-CF₃ had an AC1 IC₅₀ value of 1.4 ± 0.2 μM with 2.9-fold selectivity over AC8.

Four additional analogs that did not fit within any of the five series described for R₁ modification are reported in the supplemental information (**Table S2**). Two analogs contain a R₁ = phenyl with R₂ as either 4-isopropoxy (**67**) or 3-CF₃ (**68**) while the other two analogs have a 2-furyl moiety at the R₁ and either H (**69**) or 4-isopropoxy (**70**). All analogs had reduced activity versus both AC1 and AC8 and were not expanded on further as full series for SAR exploration.

Table 5. SAR for combined modifications



Compd	R ₁ ^a	R ₂	AC1 IC ₅₀ ^{b,c}	AC8 IC ₅₀ ^{b,c}	Fold selectivity ^d
58	A	3-CH ₃ -5-CF ₃	9.1 ± 3.0	2.4 ± 0.1	0.26
59	A	3-CF ₃ -4-CH ₃	26 ± 11	13 ± 2	0.5
60	A	3-OCH ₃ -5-CF ₃	9.4 ± 1.0	10 ± 0.4	1.1
61	D	3-CH ₃ -5-CF ₃	1.4 ± 0.2	4.1 ± 0.4	2.9
62	D	3-CF ₃ -4-CH ₃	4.6 ± 2.0	9.0 ± 5.0	1.9
63	D	3-OCH ₃ -5-CF ₃	5.0 ± 0.8	29 ± 1	5.8
64	E	3-CH ₃ -5-CF ₃	9.6 ± 1	15 ± 2	2.9
65	E	3-CF ₃ -4-CH ₃	3.7 ± 1.0	7.0 ± 1.0	1.9
66	E	3-OCH ₃ -5-CF ₃	4.8 ± 1.0	9.0 ± 1.0	1.9

^a R₁ modifications corresponding to each letter shown in Fig. 2. ^b IC₅₀ values (μM) represent the mean and SEM for three independent experiments. ^c If analog exhibits > 50% inhibition at 30 μM concentration, the IC₅₀ value was reported. If molecules exhibit < 50% inhibition then the data is listed as not determined (ND) with the percentage inhibition shown in parentheses, ND (XX%). ^d Fold selectivity = AC8 IC₅₀ / AC1 IC₅₀. If the AC8 IC₅₀ value of the compound is ND, then 30 μM used for the AC8 IC₅₀ value to calculate the fold selectivity that is shown with a > symbol.

Selectivity versus two other AC isoforms was evaluated for a subset of analogs. AC1 and AC8 represent group 1 ACs that are stimulated by Ca²⁺/calmodulin binding. We explored activity of the oxadiazole analogs against a group 2 AC (AC2, stimulated by protein kinase C) and a group 3 AC (robustly stimulated by forskolin) to assess the scaffolds effects on other AC group subtypes. Analogs **6**, **7**, **11**, **21**, **23**, **33**, and **37** were tested at single-dose (30 μM, n = 3) and compared to DMSO-controls (normalized to 100% activity). The

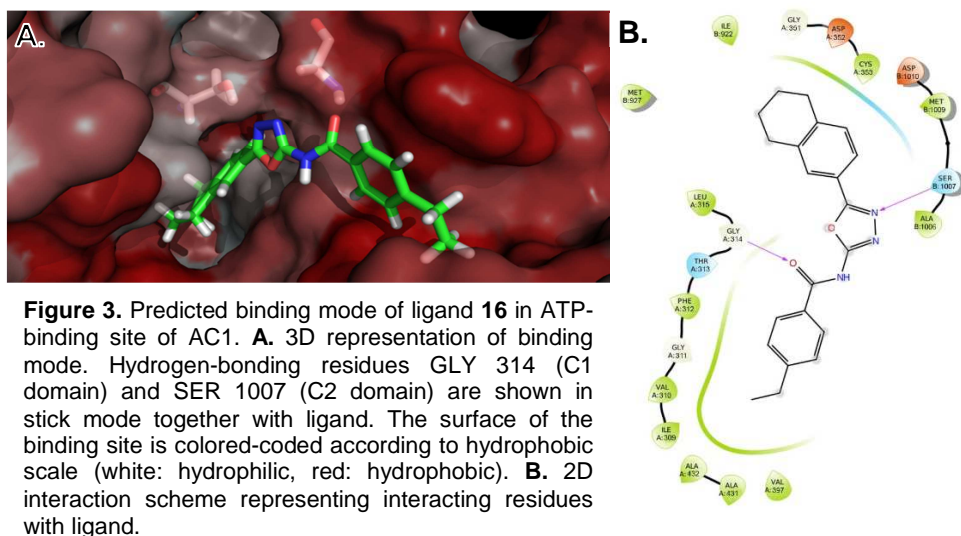
seven analogs tested exhibited roughly 2 – 4-fold increases in cAMP levels from AC2 and 1 – 2-fold increase in cAMP levels from AC5 (**Table S5**). This data suggests that the oxadiazole series potentiates AC2-mediated cAMP production and to a lesser degree AC5-mediated cAMP production.

We also compared the activity of analog **6** with SQ22536 in a novel cell model [29]. HEK-AC Δ 3/6 cells transiently transfected with AC1 [29] were incubated with test compounds in the presence of three concentrations of forskolin (3, 10 and 30 μ M). Compound **6** displayed increased inhibitory activity with increasing concentrations of forskolin (**Fig. S1**) similar to the P-site inhibitor, SQ22536. However, further pharmacological testing is necessary to validate this hypothesis and will be carried out in future work.

To assess how the molecules may interact with the cellular target we tracked the efficiency metric Lipophilic Ligand Efficiency (LLE = pIC₅₀ – Log P) [30], which provides an indication of the degree of entropic driven (hydrophobic) binding [31, 32]. Our analogs are not at “lead” status, but rather at the beginning stages of hit optimization, and possess LLE values ranging from -1.14 up to 2.90 (**Table S3**) indicating the molecules likely bind predominantly via hydrophobic interactions. To determine LLE for each molecule the Log P values for the oxadiazole analogs were calculated using MarvinSketch (version 15.9.14, ChemAxon, <http://www.chemaxon.com>).

2.4. Docking of 1,3,4-Oxadiazole Series into an AC1 Homology Model

The structure of transmembrane ACs consist of a N-terminus, two membrane domains of six-spanning helices and two cytosolic domains (C1 and C2 domains) [33]. The ATP and forskolin binding sites are found at the interface of the C1 and C2 domains of the AC [34]. Due to the lack of a human transmembrane AC crystal structure we constructed a homology model of the C1 and C2 domains of human AC1 based on the X-ray structures of the cytosolic domains of other two other mammalian ACs (PDB ID: 1AZS and 3C16) – similar to a previous AC homology model developed by our team [35]. We then utilized this model to



perform docking experiments with the analogs into both the forskolin and ATP binding sites.

Analyses of the docking results revealed significant variability among the top poses for the 60 ligands. Furthermore, for most ligands, similar scores for different binding poses were identified, which is not surprising considering the potency of the ligands is in the μM -affinity range and the significant size of the extended binding pocket. Thus, we performed clustering over all poses for all the analogs to identify the most prevalent binding mode represented by the largest cluster of poses.

The largest cluster in the forskolin binding site contained 244 poses from 32 ligands. For the ATP-binding site, two large clusters were identified with 285 poses (47 ligands) and 265 poses (46 ligands), respectively. As the average docking score for the largest cluster was also the most favorable among all three large clusters, the poses within this ATP-binding site cluster were considered to represent the most likely mode of interaction of the oxadiazole series with AC1 if the molecules were to engage the target in cells. **Figure 3** highlights the dominant interactions of a representative compound **16** with AC1 in the predicted binding mode. The 3-dimensional representation indicates the binding site is mostly hydrophobic (**Fig. 3A**). The R_2 substituents (depicted by an ethyl group in the figure) fits into a shallow hydrophobic pocket. The binding pose also suggests that only one meta-position can accommodate a substitution without sacrificing binding. If the molecules engage AC1 in cells, *and* this binding mode is accurate, this may explain why the 3,5-substituted analogs did not provide improved potencies. The 2-dimensional interaction map (**Fig. 3B**) suggests the central hydrophilic core interacts via hydrogen bonds with the backbone of GLY 314 in the C1 domain and with the hydroxyl group of SER 1007 of the C2 domain. The terminal hydrophobic ligand moieties are enclosed by hydrophobic regions including residues ILE 309, VAL 310, GLY 311, PHE 312, VAL 397, ALA 431, ALA 432 (all in the C1 domain) for the R_2 substituents and LEU 315, GLY 351 (both in the C1 domain), ILE 922 and MET 927 (both in the C2 domain) for the R_1 substituents. The docking data supports the hypothesis that these molecules bind to their targets via predominantly hydrophobic interactions. Additionally, the data indicates that there is a higher probability the 1,3,4-oxadiazole series would bind within the ATP-binding site of AC1 rather than the forskolin binding site.

2.5. Cell viability

In parallel to the assessment of the effects of the compounds on cAMP accumulation in the HEK cell lines stably expressing AC1 and AC8, the toxicity of the molecules was also examined. Upon a single dose (30 μ M), the viability of the cells was determined after incubation for 90 minutes with the analogs using a luminescent reporter for the metabolic marker ATP, and % cell viability determined compared to DMSO (100% viable) and Triton-X (0% viable) treated controls (**Table S4**). The results indicated little to no potential toxic liability for the 1,3,4-oxadiazole series as the overwhelming majority of molecules exhibited cell viability greater than 80%. Only three of the reported analogs displayed lower cell viability below 80% (**44** – 71%; **68** – 78%; **69** – 73%).

2.6. *In vivo efficacy in a mouse model of inflammatory pain.*

Based on the pharmacological profile combining low micromolar potency, moderate selectivity over AC8, and mid-range LLE compared to similarly potent analogs we next assessed the ability of (**61**) to provide analgesia in an inflammatory pain model in C57BL/6 mice. Intraplantar injection of CFA (Complete Freund's adjuvant) induced robust mechanical hypersensitivity the following day in the

ipsilateral paw (**Fig. 4A**, CFA day2, filled symbols) as evidenced by mice withdrawing their paw upon tactile stimulation with von Frey filaments of lower diameter and force than when stimulating the contralateral paw (**Fig. 4A**, day2, open symbols). Following the measurement of CFA induced hypersensitivity on day 2, mice received a systemic intraperitoneal (*i.p.*) injection of 5 mg/kg of compound **61** or vehicle and mechanical sensitivity was recorded 30 minutes post-injection. Two-way repeated measure ANOVA revealed a significant effect of treatment ($F_{1,36} = 113.3$, $p < 0.0001$) and interaction ($F_{3,36} = 4.272$, $p = 0.011$). Post-hoc Bonferroni analysis revealed that analog **61** ($t = 3.17$, $p < 0.05$) but not vehicle ($t = 0.244$, $p > 0.05$) significantly attenuated, the hypersensitivity in the ipsilateral paw without significantly altering response in the contralateral

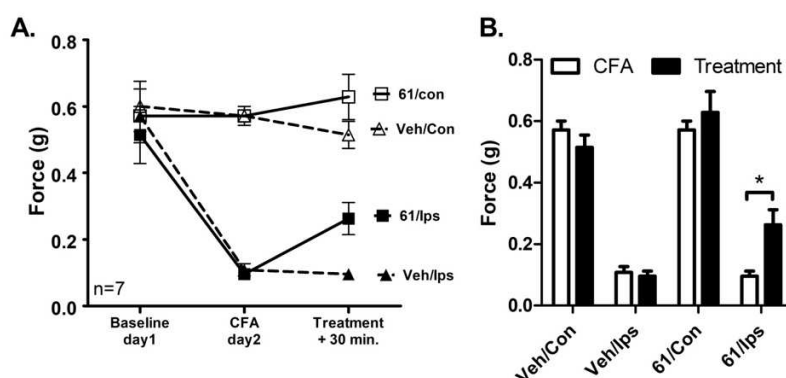


Figure 4. Efficacy of **61** in mouse inflammatory pain model. **A.** Time course of induction and treatment of inflammatory mechanical hypersensitivity: Male C57BL/6 mice ($n=7$) were injected with CFA in the ipsilateral paw (lps, closed symbols) and paw sensitivity was measured in the ipsilateral and contralateral paw (Con, open symbols). On day 2 mice received an *i.p.* injection of vehicle (veh, triangles) or 5 mg/kg **61** (squares). **B.** Statistical analysis of drug/vehicle treatment (filled bars) on CFA induced mechanical hypersensitivity (open bars) of contralateral and ipsilateral paws. $**P < 0.01$ (Two-way repeated measure ANOVA with Bonferroni test). The data shown represent the average and SEM of each group of measurements.

paw (**Fig. 4B**). The effect of **61** was short-lived and mice regained the hypersensitivity in their ipsilateral paw the following day (data not shown).

3. Discussion

With the recent genetic and pharmacologic evidence suggesting inhibition of AC1 activity may be a viable strategy for treatment of chronic inflammatory and neuropathic pain, our team set out to discover novel small molecules that may be used to validate this strategy for pain therapy. A high-throughput screen in search of small molecules that reduce Ca^{2+} /calmodulin-mediated cAMP accumulation in HEK cells stably expressing AC1 was carried out. The 1,3,4-oxadiazole series was identified as a hit scaffold (represented by **1**) and its activity was validated in further cellular cAMP accumulation assays against AC1 and AC8. We then embarked upon a SAR optimization campaign to improve potency toward AC1 and/or selectivity over AC8. In total, 65 new 1,3,4-oxadiazole containing analogs were designed and synthesized incorporating five common R_1 elements observed in the HTS hits. During optimization there were modest gains in potency versus AC1 and selectivity over AC8, albeit not to the desired sub-micromolar level for AC1 potency or the > 10 -fold selectivity over AC8. Nonetheless, there were some SAR trends that were observed from this structural class. In particular, SAR at the R_2 position revealed that substitution with the same functional group at the meta-position was favored over the para-position for AC1 potency as illustrated by comparison of **10** (3- OCH_3) vs **12** (4- OCH_3), **14** (3-F) vs **13** (4-F), and **38** (3-F) vs **39** (4-F). This trend could be observed in the combined modifications as well in which **58** (3- CH_3 -5- CF_3) outperformed **59** (3- CF_3 -4- CH_3) and **61** (3- CH_3 -5- CF_3) outperformed **62** (3- CF_3 -4- CH_3). However, in the combined modification analogs there was an exception to this observation in which the 3,4-di-substitution was modestly more potent than the 3,5 when combined with the cyclohexyl moiety at the R_1 (**65** and **64**, respectively), suggesting that the favored meta- substitution is best when combined with an appropriate R_1 substitution. The preference of functional group at on the R_2 side of the molecule is less clear. There appears to be a slight preference for halogenated moieties especially fluorine containing substituents. However, two series (D and E) had the introduction of an aromatic phenyl substituent at R_2 , and these typically boosted AC1 potency compared to the rest of the analogs within those series.

There were clear preferences in the R_1 functional groups that could be observed during our SAR analysis. Analogs containing either 2,3-dihydro-1,4-dioxin-6-yl (B-series) or 2-thiophene (C-series) consistently underperformed in terms of AC1 potency when compared to their counterparts from the A, D, and E-series.

Thus, analogs for the B and C series were deprioritized in our design. Direct comparison of R_2 moieties between series, R_1 = 5,6,7,8-tetrahydronaphthalene (A-series) consistently outperformed the 4-F-phenyl (D-series) and cyclohexyl (E-series) in terms of AC1 potency. The A-series also produced the most selective molecules when comparing fold-selectivity over AC8. Given that we only determined IC_{50} values for molecules that displayed $\geq 50\%$ inhibition at 30 μM we were not able to determine a large number of IC_{50} values against AC8, thus comparison of selectivity is partially incomplete without full IC_{50} values against both isoforms. When comparing % inhibition of AC8 across each series the cyclohexyl R_1 may potentially display similar selectivity toward to AC1, however, this is only an estimation and appears to come at the detriment of AC1 potency.

The 5,6,7,8-tetrahydronaphthalene proved to be the best when comparing analogs between series, however, to our surprise the selectivity of this R_1 moiety was not retained when paired with the combined R_2 modifications suggesting the combination of R_1 with specific R_2 moieties are necessary to maintain or improve AC1 selectivity over AC8. In fact, the most potent and selective analogs in the combined sets belong to the R_1 = 4-F-phenyl (D-series), however, most analogs exhibited similar AC1 and AC8 potency. Thus, it is difficult to deduce any SAR trends from these combined modifications without further investigation.

Even though there are some trends to be observed the overall SAR is relatively “flat” as almost all analogs remained in the 1 to 30 μM range for AC1 potency. To this point we have not tested any analogs that exhibited significant improvement in AC1 potency or selectivity attributable to a particular substituent. Alternatively, only two analogs exhibited a reduction of potency toward AC1 beyond 30 μM . This flat SAR may indicate that the molecules may bind to the cellular target predominantly via non-specific hydrophobic interactions. The relatively high LogP for this scaffold series would support this assertion as increased LogP tends to result in an increased interaction with hydrophobic protein surfaces [36]. In fact, the A-series of molecules, containing the 5,6,7,8-tetrahydronaphthalene at the R_1 position, were on average the most potent toward AC1 (average AC1 IC_{50} value of 4.3 μM) and possessed the highest average LogP (average LogP = 5.65, calculated using ChemDraw v17). As described above, tracking the efficiency metric Lipophilic Ligand Efficiency (LLE = pIC_{50} – Log P) [30], provides an indication of the degree of entropic driven (hydrophobic) binding [31, 32]. Acceptable LLE values for lead candidates for clinical evaluation is > 5 , with a positive correlation to increased enthalpic (specific, polar interactions) binding energy [30]. Our analogs are not yet to lead status, but rather at the beginning stages of hit optimization, and possess LLE values ranging from -1.14

up to 2.90. These values indicate the molecules most likely bind predominantly via hydrophobic interactions. While this is not an attribute that disqualifies these molecules from further development it does indicate that more emphasis should be placed on incorporating hydrogen-bond donors and acceptors capable of forming polar interactions within the active site. Nonetheless, the 1,3,4-oxadiazoles still represent an expansion of the known chemical space for AC1 inhibitors and there are clear areas that can be targeted for improvement on this scaffold in the next phase of the project.

After evaluation of all analogs in the cellular models we chose to test one analog from our study in an *in vivo* mouse model to evaluate for its efficacy to attenuate inflammatory pain. While it would be desirable to have a highly selective AC1 molecule, the AC1 inhibitor NB001 – that has moderate selectivity for AC1 over AC8 (10-fold) – has displayed analgesic effects in various models of neuropathic and inflammatory pain [22, 37, 38]. Therefore, we selected analog **61** due to its low- μM potency against cellular AC1 activity (IC_{50} value of 1.4 μM), moderate selectivity over AC8 (2.9-fold), and mid-range LLE compared to the entire analog set (1.29). The molecule dosed at 5 mg/kg *i.p.* provided a modest, but significant analgesic effect in the CFA model as mice exhibited a significantly reduced allodynia compared to the vehicle control. A higher dose may provide a greater analgesic effect, however, due to the limited solubility of the molecule, we were not able to increase dosage. The scaffold also potentiates cAMP production from AC2 and AC5, however, these AC isoforms are not directly involved in signaling pathways associated with chronic pain. Therefore, we propose that the *in vivo* efficacy observed in this experiment is a result of AC1 inhibition and not related to the effects at AC2 or AC5. Regardless, the preliminary results for this scaffold in the treatment of chronic pain are promising and warrant further investigation.

Because the Ca^{2+} /calmodulin-mediated AC1 and AC8 cAMP production is the output for evaluation of our molecules we should stress that this is a cellular assay and does not necessarily indicate the molecules are engaging AC1 or AC8 in the cells. The possibility remains that these molecules may be leading to decreased cAMP production via an alternative pathway, similar to what has been suggested for NB001 [23]. Additionally, simply expressing and purifying recombinant human AC isoforms for *in vitro* binding analysis remains extremely difficult. Even though direct target engagement has not been completely verified in our system at this point we chose to make an educated suggestion as to the potential AC1 binding site if engagement is indeed taking place in the cells. The AC1 homology model suggests the analogs would

preferentially bind into a hydrophobic region of the ATP-binding site, which aligns with the observation that increased hydrophobicity provides the greatest AC1 potency. However, further experiments are necessary to validate these proposed binding interactions. Nonetheless, the desired goal is to reduce cAMP levels mediated through AC1 activity in the cellular context, and these HEK cell lines express the AC1 or AC8 isoforms at much higher levels relative to other AC isoforms. Therefore, the reduction in cAMP levels can be attributed mostly to inhibition of the respective isoform, whether it be a result of direct engagement with AC1 or through an alternative mechanism. Further studies will be done to pharmacologically evaluate this series, validate the intracellular target and assess activity against other AC isoforms as part of future research.

4. Conclusions

Our team reports a novel class of 1,3,4-oxadiazole containing compounds that inhibit Ca^{2+} /calmodulin-stimulated cAMP production mediated by AC1 with varying selectivity over AC8. An SAR study has identified functional group substitution patterns that provide either greater potency toward AC1 or greater selectivity for AC1 over AC8. Primarily, substitution at the meta-position of the R_2 side were consistently more potent than the respective para-substitution. In addition, and among the substitutions investigated, halogen containing functional groups also seemed to be preferred. We found that $\text{R}_1 = 5,6,7,8\text{-tetrahydronaphthalene}$ (A-series) was the most potent moiety on the left-hand side of the molecule and this may be attributed to increased non-specific, hydrophobic binding rather than productive interactions with the protein surface. Future medicinal chemistry on this class will focus on introducing more polar functionalities to the molecule. Because our initial SAR maintained R_1 substitutions that were present in the HTS hit deck, future diversification at this position may provide improved physicochemical and inhibitory properties. Nonetheless, one molecule, **61**, was tested for efficacy in a mouse model of inflammatory pain and was observed to provide a modest, yet significant, analgesic effect compared to controls consistent with the current hypothesis that AC1 is a viable target to treat chronic pain. Since the series was not fully selective toward AC1 but also exhibited potency toward AC8 further exploration into potential side effects in learning and memory may be warranted. Previously reported AC1 inhibitors, such as NB001 and ST034307, have exhibited either greater potency toward AC1 and/or selectivity over other AC isoforms with greater efficacy in animal pain models than our molecules [22, 24]. However, both molecules have drawbacks with respect to their potential for further development while the 1,3,4-oxadiazole scaffold has proven to be amenable for optimization. Therefore, based on our initial SAR and *in vivo* results,

our team remains enthusiastic about the potential of the 1,3,4-oxadiazole scaffold as a promising new class of AC1 inhibitors for the treatment of chronic pain.

5. Experimental

5.1. Chemistry

5.1.1. General

The purity of all final compounds was >95 % purity as assessed by HPLC. Final compounds were analyzed on an Agilent 1200 series chromatograph. The chromatographic method utilized as ThermoScientific Hypersil GOLD C-18 4.6 x 250 mm, 3 μ m column. UV detection wavelength = 220 nm; flow-rate = 1.0 mL/min; gradient = 5 – 95% acetonitrile over 12 min and 3 min hold time at 95% acetonitrile. Both organic and aqueous mobile phases contain 0.1% v/v formic acid. The mass spectrometer used is an AB Sciex 4500 QTrap triple-quadrupole mass spectrometer with an ESI source or an Advion CMS-L Compact Mass Spectrometer with an ESI or an APCI source. Samples are submitted for analysis solubilized in 1:1 acetonitrile:water solution or using the atmospheric solids analysis probe (ASAP). ^1H and ^{13}C NMR spectra were recorded on either Bruker DRX500 spectrometer (operating at 500 and 125 MHz, respectively) or Bruker AVIII (operating at 800 and 200 MHz, respectively) in $\text{DMSO}-d_6$ or CDCl_3 with or without the internal standard of TMS at 0.05% v/v. The chemical shifts (δ) reported as parts per million (ppm) and the coupling constants are reported as s = singlet, bs = broad singlet, d = doublet, t = triplet, q = quartet, dd = doublet of doublet, m = multiplet. Compounds were generally prepared according to scheme 1 and protocols are detailed below. Intermediate **4C** was commercially available.

5.1.2. General procedure for synthesis of hydrazine-carboxamide intermediates (**3**).

(*E*)-2-((5,6,7,8-tetrahydronaphthalen-2-yl)methylene)hydrazine-1-carboxamide (**3A**).

To a vial was added the semicarbazide hydrochloride (0.73 g, 6.5 mmol, 1.0 eq.) and sodium acetate (1.07 g, 13.1 mmol, 2.0 eq.) followed by water (10 mL). To a second vial was added the 5,6,7,8-tetrahydronaphthalene-2-carbaldehyde (**2A**, 1.05 g, 6.5 mmol, 1.0 eq.) and methanol (10 mL). The aldehyde

solution was then added dropwise to the first solution while stirring at room temperature. The reaction stirred for 30 min in which time it formed a suspension. The solid was filtered out by vacuum filtration to produce **3A** (1.36 g, 6.26 mmol, 96%) as a white solid. ^1H NMR (500 MHz, DMSO- d_6): δ 10.13 (s, 1H), 7.77 (s, 1H), 7.42 (dd, J = 7.9, 1.8 Hz, 1H), 7.38 (s, 1H), 7.06 (d, J = 7.9 Hz, 1H), 6.42 (s, 2H), 2.77 – 2.69 (m, 4H), 1.78 – 1.69 (m, 4H).

5.1.3. *(E)*-2-((2,3-dihydrobenzo[*b*][1,4]dioxin-6-yl)methylene)hydrazine-1-carboxamide (**3B**).

Prepared using the same procedure as molecule **3A** with semicarbazide hydrochloride (0.13 g, 1.1 mmol, 1.0 eq.), sodium acetate (0.19 g, 2.3 mmol, 2.0 eq.) in water (1 mL) and 2,3-dihydrobenzo[*b*][1,4]dioxine-6-carbaldehyde (**2B**, 0.19 g, 1.1 mmol, 1.0 eq.) in methanol (1 mL) to produce **3B** (0.23 g, 1.0 mmol, 92%) as a white solid. ^1H NMR (500 MHz, DMSO- d_6): δ 10.08 (s, 1H), 7.71 (s, 1H), 7.29 (d, J = 1.8 Hz, 1H), 7.14 (dd, J = 8.3, 1.8 Hz, 1H), 6.85 (br s, J = 8.3 Hz, 1H), 6.44 (d, J = 17.6 Hz, 2H), 4.26 (s, 4H).

5.1.4. *(E)*-2-(4-fluorobenzylidene)hydrazine-1-carboxamide (**3D**).

Prepared using the same procedure as molecule **3A** with semicarbazide hydrochloride (0.88 g, 7.9 mmol, 1.0 eq.), sodium acetate (1.3 g, 16 mmol, 2.0 eq.) in water (10 mL) and 4-fluorobenzaldehyde (**2D**, 0.98 g, 7.9 mmol, 1.0 eq.) in methanol (10 mL) to produce **3D** (1.23 g, 6.8 mmol, 86%) as a white solid. ^1H NMR (500 MHz, DMSO- d_6): δ 10.24 (s, 1H), 7.83 (s, 1H), 7.80 (d, J = 8.8 Hz, 1H), 7.79 (d, J = 8.9 Hz, 1H), 7.23 (d, J = 8.9 Hz, 1H), 7.22 (d, J = 8.8 Hz, 1H), 6.50 (s, 2H).

5.1.5. *(E)*-2-(cyclohexylmethylene)hydrazine-1-carboxamide (**3E**).

Prepared using the same procedure as molecule **3A** with semicarbazide hydrochloride (0.57 g, 5.1 mmol, 1.0 eq.), sodium acetate (0.84 g, 10 mmol, 2.0 eq.) in water (10 mL) and cyclohexanecarbaldehyde (**2E**, 0.57 g, 5.1 mmol, 1.0 eq.) in methanol (10 mL) to produce **3E** (0.74 g, 4.4 mmol, 85%) as a white solid. ^1H NMR (500 MHz, DMSO- d_6): δ 9.70 (s, 1H), 7.01 (d, J = 5.2 Hz, 1H), 6.07 (s, 1H), 2.13 – 2.01 (m, 1H), 1.72 – 1.60 (m, 5H), 1.61 – 1.52 (m, 1H), 1.25 – 1.08 (m, 6H).

5.1.6. General procedure for synthesis of 2-amino-1,3,4-oxadiazole intermediates (**4**).

5-(5,6,7,8-tetrahydronaphthalen-2-yl)-1,3,4-oxadiazol-2-amine (4A).

To a vial was added **3A** (0.18 g, 0.81 mmol, 1.0 eq.), sodium acetate (0.13 g, 1.62 mmol, 2.0 eq.) and acetic acid (0.5 mL). To a second vial was added the bromine (0.14 g, 0.89 mmol, 1.1 eq.) in acetic acid (0.5 mL). The bromine solution was then added to the first vial while stirring in a dropwise manner at room temperature. The reaction was then heated to 60 °C and stirred for 1 hour. The reaction was then cooled to room temperature and poured onto ice water. A yellow precipitate formed and was filtered by vacuum filtration then rinsed with DCM to provide **4A** (0.16 g, 0.77 mmol, 95%) as a pale yellow solid. ¹H NMR (500 MHz, DMSO-*d*₆): δ 7.53 – 7.45 (m, 2H), 7.31 (br s, 2H), 7.20 (d, *J* = 7.9 Hz, 1H), 2.83 – 2.70 (m, 4H), 1.81 – 1.70 (m, 4H).

*5.1.7. 5-(2,3-dihydrobenzo[*b*][1,4]dioxin-6-yl)-1,3,4-oxadiazol-2-amine (4B).*

Prepared using the same procedure as molecule **4A** with **3B** (0.49 g, 2.24 mmol, 1.0 eq.) and sodium acetate (0.37 g, 4.48 mmol, 2.0 eq.) in acetic acid (1.0 mL). A second vial of bromine (0.39 g, 2.46 mmol, 1.1 eq.) in acetic acid (0.5 mL). Produced **4B** (0.38 g, 1.75 mmol, 78%) as a pale red solid. ¹H NMR (500 MHz, DMSO-*d*₆): δ 7.67 (s, 2H), 7.29 (dd, *J* = 8.4, 2.1 Hz, 1H), 7.23 (d, *J* = 2.1 Hz, 1H), 7.02 (d, *J* = 8.4 Hz, 1H), 4.34 – 4.29 (m, 4H).

5.1.8. 5-(4-fluorophenyl)-1,3,4-oxadiazol-2-amine (4D).

Prepared using the same procedure as molecule **4A** with **3D** (0.50 g, 2.7 mmol, 1.0 eq.) and sodium acetate (0.44 g, 5.4 mmol, 2.0 eq.) in acetic acid (2.0 mL). A second vial of bromine (0.43 g, 2.7 mmol, 1.1 eq.) in acetic acid (1.0 mL). Produced **4D** (0.39 g, 2.2 mmol, 81%) as a white solid. ¹H NMR (500 MHz, DMSO-*d*₆): δ 7.86 – 7.74 (m, 2H), 7.40 – 7.31 (m, 2H), 7.23 (s, 2H).

5.1.9. 5-cyclohexyl-1,3,4-oxadiazol-2-amine (4E).

Prepared using the same procedure as molecule **4A** with **3E** (0.18 g, 1.1 mmol, 1.0 eq.) and sodium acetate (0.17 g, 2.1 mmol, 2.0 eq.) in acetic acid (1.0 mL). A second vial of bromine (0.19 mL, 1.2 mmol, 1.1 eq.) in acetic acid (0.5 mL). Produced **4E** (0.15 g, 0.87 mmol, 83%) as a pale yellow solid. ¹H NMR (500 MHz,

DMSO- d_6): δ 6.82 (s, 2H), 2.71 (tt, J = 10.9, 3.6 Hz, 1H), 1.95 – 1.87 (m, 2H), 1.75 – 1.68 (m, 2H), 1.67 – 1.58 (m, 1H), 1.48 – 1.29 (m, 4H), 1.28 – 1.20 (m, 1H).

5.1.10. *General procedure “A” using a commercially available acyl chloride for amide coupling.

N-(5-(5,6,7,8-tetrahydronaphthalen-2-yl)-1,3,4-oxadiazol-2-yl)benzamide (**1**).

To a vial was added the **4A** (0.030 g, 0.14 mmol, 1.0 eq.) followed by pyridine (0.6 mL) and 4-benzoyl chloride (0.020 g, 0.14 mmol, 1.0 eq.) at room temperature. The reaction stirred for 18 hours then was poured into ice water and a precipitate formed. This precipitate was filtered by vacuum filtration and was further purified by reverse-phase flash chromatography (5 – 100% MeCN:water). All fractions containing the desired product were isolated and concentrated to produce **1** (0.028 g, 0.084 mmol, 40%) as a pale yellow solid. ^1H NMR (500 MHz, CDCl_3): δ 12.21 (br s, 1H), 8.26 (d, J = 7.7 Hz, 2H), 7.84 – 7.74 (m, 2H), 7.62 (t, J = 7.3 Hz, 1H), 7.53 (t, J = 7.5 Hz, 2H), 7.19 (d, J = 7.8 Hz, 1H), 2.89 – 2.79 (m, 4H), 1.89 – 1.79 (m, 4H). ^{13}C NMR (200 MHz, DMSO- d_6): δ 165.0, 161.5, 157.7, 141.1, 137.9, 132.9, 132.2, 130.0, 128.6, 128.3, 126.5, 123.1, 120.5, 28.84, 28.58, 22.35, 22.30. ESI-MS: m/z 319.7 $[\text{M} + \text{H}]^+$; HPLC retention time: 12.940 min. HPLC purity 96.5%.

5.1.11. *General procedure “B” using the commercially available carboxylic acid for amide coupling.

N-(5-(5,6,7,8-tetrahydronaphthalen-2-yl)-1,3,4-oxadiazol-2-yl)-3-(trifluoromethyl)benzamide (**6**).

Step 1: To a vial was added the 3-trifluoromethylbenzoic acid (0.044 g, 0.23 mmol, 1.0 eq.) in DCM (0.5 mL) followed by 1 drop of DMF. The reaction was then cooled to 0 °C followed by slow addition of oxalyl chloride (0.023 mL, 0.27 mmol, 1.2 eq.). The reaction then was allowed to warm to room temperature and stir for 1 hour. After 1 hour the reaction was concentrated *in vacuo* and carried into the amide coupling reaction without purification or characterization.

Step 2: To a vial was added the **4A** (0.050 g, 0.23 mmol, 1.0 eq.) followed by pyridine (0.3 mL). To the vial containing the 3-trifluoromethylbenzoyl chloride (carried over from previous step) was add pyridine (0.3 mL) to form a suspension. The acyl chloride suspension was added to the first vial while stirring at room temperature. The reaction stirred for 18 hours then was poured into ice water and a precipitate formed. This precipitate was filtered by vacuum filtration and was further purified by normal phase flash chromatography (0 – 5% MeOH:DCM). All fractions containing the desired product were isolated and concentrated to produce **6**

(0.14 g, 0.035 mmol, 15%). ^1H NMR (500 MHz, CDCl_3): δ 12.72 (s, 1H), 8.41 (s, 1H), 8.34 (d, $J = 7.9$ Hz), 8.04 (d, $J = 7.9$ Hz), 7.82 (t, $J = 7.8$ Hz, 1H), 7.74 – 7.62 (m, 2H), 7.29 (d, $J = 7.9$ Hz, 1H), 2.85–2.78 (m, 4H), 1.85 – 1.72 (m, 4H). ^{13}C NMR (200 MHz, $\text{DMSO}-d_6$): δ 167.8, 166.4, 160.6, 141.3, 138.4, 132.9, 132.0, 130.5, 130.3, 130.1, 129.6 (q, $J = 32.0$ Hz), 129.1, 126.8, 126.1 (q, $J = 270.0$ Hz), 123.5, 121.3, 29.3, 29.1, 22.9, 22.8. ESI-MS: 387.9 $[\text{M} + \text{H}]^+$. HPLC retention time: 13.813 min. HPLC purity 95.5%.

5.1.12. *N*-(5-(5,6,7,8-tetrahydronaphthalen-2-yl)-1,3,4-oxadiazol-2-yl)-4-(bromo)benzamide (**7**).

Prepared using general procedure *B* with 4-bromobenzoic acid (0.051 g, 0.26 mmol, 1.1 eq.), oxalyl chloride (0.023 mL, 0.27 mmol, 1.15 eq.), **4A** (0.050 g, 0.23 mmol, 1.0 eq.), and pyridine (1.0 mL) to produce **7** (0.049 g, 0.117 mmol, 50%) as a light pink solid. ^1H NMR (500 MHz, CDCl_3): δ 12.04 (s, 1H), 8.12 (d, $J = 8.5$ Hz, 2H), 7.78 – 7.71 (m, 2H), 7.70 – 7.59 (m, 2H), 7.21 (d, $J = 8.1$ Hz, 1H), 2.89 – 2.78 (m, 4H), 1.86 – 1.83 (m, 4H). HPLC retention time: 13.657 min. HPLC purity 95.3%.

5.1.13. *N*-(5-(5,6,7,8-tetrahydronaphthalen-2-yl)-1,3,4-oxadiazol-2-yl)-4-(isopropoxy)benzamide (**8**).

Prepared using general procedure *A* with **4A** (0.050 g, 0.23 mmol, 1.0 eq.), 4-isopropoxybenzoyl chloride (0.062 g, 0.32 mmol, 1.4 eq.), and pyridine (1.0 mL) to produce **8** (0.010 g, 0.027 mmol, 12%). ^1H NMR (800 MHz, $\text{DMSO}-d_6$): δ 8.00 – 7.98 (m, 2H), 7.66 – 7.64 (m, 1H), 7.64 – 7.62 (m, 1H), 7.27 – 7.24 (m, 1H), 7.05 – 7.03 (m, 2H), 4.75 (p, $J = 6.0$ Hz, 1H), 2.82 – 2.75 (m, 4H), 1.77 – 1.73 (m, 4H), 1.29 (d, $J = 6.0$ Hz, 6H). ^{13}C NMR (200 MHz, CDCl_3): δ 165.2, 161.7, 158.7, 141.4, 138.3, 130.9, 130.5, 126.9, 124.6, 123.5, 121.1, 115.51, 70.1, 29.3, 29.1, 22.8, 22.8, 22.2. ESI-MS: m/z 378.0 $[\text{M} + \text{H}]^+$; HPLC retention time: 13.629 min. HPLC purity 97.9%.

5.1.14. *N*-(5-(5,6,7,8-tetrahydronaphthalen-2-yl)-1,3,4-oxadiazol-2-yl)-3-(thiomethoxy)benzamide (**9**).

Prepared using general procedure *B* with 3-thiomethoxybenzoic acid (0.026 g, 0.26 mmol, 1.1 eq.), oxalyl chloride (0.015 mL, 0.17 mmol, 1.2 eq.), **4A** (0.030 g, 0.14 mmol, 1.0 eq.), and pyridine (1.0 mL) to produce **9** (0.015 g, 0.047 mmol, 26%). ^1H NMR (800 MHz, CDCl_3): δ 8.07 (s, 1H), 7.97 (d, $J = 7.7$ Hz, 1H), 7.79 (s, 2H), 7.53 – 7.41 (m, 2H), 7.20 (d, $J = 8.4$ Hz, 1H), 2.89 – 2.82 (m, 4H), 2.55 (s, 3H), 1.88 – 1.79 (m, 4H). ^{13}C NMR (200 MHz, CDCl_3): δ 142.0, 140.0, 138.2, 130.8, 129.9, 129.0, 127.3, 126.2, 125.3, 123.7, 120.2,

29.6, 29.3, 22.9, 22.8, 15.6. ESI-MS: m/z 366.0 $[M + H]^+$, 388.0 $[M + Na]^+$; HPLC retention time: 13.511 min. HPLC purity 95.8%.

5.1.15. *N*-(5-(5,6,7,8-tetrahydronaphthalen-2-yl)-1,3,4-oxadiazol-2-yl)-3-(methoxy)benzamide (**10**).

Prepared using general procedure *B* with 3-methoxybenzoic acid (0.042 g, 0.28 mmol, 1.2 eq.), oxalyl chloride (0.027 mL, 0.32 mmol, 1.4 eq.), **4A** (0.049 g, 0.23 mmol, 1.0 eq.), and pyridine (2.0 mL) to produce **10** (0.031 g, 0.088 mmol, 39%) as a white solid. ^1H NMR (800 MHz, DMSO- d_6): δ 12.11 (s, 1H), 7.76 – 7.53 (m, 4H), 7.46 (t, J = 7.9 Hz, 1H), 7.30 – 7.15 (m, 2H), 3.83 (s, 3H), 2.83 – 2.68 (m, 4H), 1.81 – 1.61 (m, 4H). ^{13}C NMR (200 MHz, DMSO- d_6): δ 165.4, 161.6, 159.7, 158.3, 141.5, 138.4, 134.2, 130.4, 130.2, 126.9, 123.5, 121.0, 121.0, 119.4, 113.5, 55.9, 29.3, 29.1, 22.8, 22.8. ESI-MS: m/z 350.1 $[M + H]^+$, 372.1 $[M + Na]^+$; HPLC retention time: 13.034 min. HPLC purity 95.2%.

5.1.16. *N*-(5-(5,6,7,8-tetrahydronaphthalen-2-yl)-1,3,4-oxadiazol-2-yl)-4-(methyl)benzamide (**11**).

Prepared using general procedure *A* with **4A** (0.040 g, 0.19 mmol, 1.0 eq.), 4-methylbenzoyl chloride (0.032 g, 0.20 mmol, 1.1 eq.), and pyridine (1.0 mL) to produce **11** (0.028 g, 0.084 mmol, 45%) as a white solid. ^1H NMR (500 MHz, DMSO- d_6): δ 12.06 (s, 1H), 7.95 (d, J = 7.9 Hz, 2H), 7.71 – 7.66 (m, 2H), 7.38 (d, J = 8.0 Hz, 2H), 7.28 (d, J = 8.0 Hz, 1H), 2.91 – 2.76 (broad m, 4H), 2.40 (s, 3H), 1.85 – 1.73 (broad m, 4H). ^{13}C NMR (126 MHz, DMSO- d_6): δ 167.4, 158.0, 143.3, 141.1, 138.0, 130.1, 129.4, 129.3, 129.2, 128.4, 126.5, 123.1, 120.6, 28.9, 28.6, 22.4, 22.4, 21.2. ESI-MS: 333.5 $[M]^+$. HPLC retention time: 13.244 min. HPLC purity 100%.

5.1.17. *N*-(5-(5,6,7,8-tetrahydronaphthalen-2-yl)-1,3,4-oxadiazol-2-yl)-4-(methoxy)benzamide (**12**).

Prepared using general procedure *A* with **4A** (0.050 g, 0.23 mmol, 1.0 eq.), 4-methoxybenzoyl chloride (0.040 g, 0.24 mmol, 1.1 eq.), and pyridine (1.0 mL) to produce **12** (0.047 g, 0.13 mmol, 58%) as a white solid. ^1H NMR (500 MHz, DMSO- d_6): δ 8.04 (d, J = 8.3 Hz, 1H), 7.91 (d, J = 8.4 Hz, 1H), 7.69 – 7.59 (m, 2H), 7.23 (dd, J = 52.5, 7.9 Hz, 1H), 7.08 (dd, J = 23.4, 8.4 Hz, 2H), 3.83 (s, 3H), 2.78 (s, 4H), 1.77 (d, J = 4.4 Hz, 4H). ^{13}C NMR (200 MHz, DMSO- d_6): δ 166.4, 165.8, 163.5, 162.5, 138.4, 137.2, 129.8, 129.5, 128.6, 126.9, 124.9,

123.6, 114.2, 56.0, 29.3, 29.3, 23.0, 22.9. APCI-MS = m/z 350.3 $[M + H]^+$. HPLC retention time: 12.242 min. HPLC purity 100%.

5.1.18. *N*-(5-(5,6,7,8-tetrahydronaphthalen-2-yl)-1,3,4-oxadiazol-2-yl)-4-(fluoro)benzamide (**13**).

Prepared using general procedure A with **4A** (0.045 g, 0.21 mmol, 1.0 eq.), 4-fluorobenzoyl chloride (0.040 g, 0.25 mmol, 1.2 eq.), and pyridine (1.0 mL) to produce **13** (0.020 g, 0.059 mmol, 28%) as a white solid. 1H NMR (500 MHz, DMSO- d_6): δ 12.10 (br s, 1H), 8.13 - 8.09 (broad m, 2H), 7.70-7.64 (broad m, 2H), 7.46 - 7.35 (broad m, 2H), 7.30-7.26 (broad m, 1H), 2.83-2.78 (broad m, 4H), 1.81-1.74 (broad m, 4H). ^{13}C NMR (200 MHz, DMSO- d_6): δ 170.6, 166.1, 165.3 (d, J = 248.0 Hz), 158.2, 141.7, 138.4, 131.7 (d, J = 8.0 Hz), 130.5, 129.5, 127.0, 123.6, 120.9, 116.2 (d, J = 22.0 Hz), 29.3, 29.1, 22.8, 22.8. ESI-MS: 338.2 $[M + H]^+$. HPLC retention time: 12.785 min. HPLC purity 97.9%.

5.1.19. *N*-(5-(5,6,7,8-tetrahydronaphthalen-2-yl)-1,3,4-oxadiazol-2-yl)-3-(fluoro)benzamide (**14**).

Prepared using general procedure A with **4A** (0.042 g, 0.20 mmol, 1.0 eq.), 3-fluorobenzoyl chloride (0.031 g, 0.20 mmol, 1.0 eq.), and pyridine (1.0 mL) to produce **14** (0.024 g, 0.071 mmol, 36%) as a white solid. 1H NMR (800 MHz, DMSO- d_6): δ 7.90 (d, J = 7.7 Hz, 1H), 7.83 (d, J = 9.8 Hz, 1H), 7.66 (d, J = 7.8 Hz, 1H), 7.65 (s, 1H), 7.62 - 7.59 (m, 1H), 7.52 - 7.48 (m, 1H), 7.28 (d, J = 7.9 Hz, 1H), 2.82 - 2.79 (broad m, 4H), 1.78-1.76 (m, 4H). ^{13}C NMR (200 MHz, DMSO- d_6): δ 165.5, 162.4 (d, J = 256.0 Hz), 160.0, 159.6, 141.4, 138.4, 136.5, 131.2 (d, J = 8.0 Hz), 130.5, 126.9, 125.0, 123.5, 121.2, 119.8 (d, J = 20.0 Hz), 115.5 (d, J = 24.0 Hz), 29.3, 29.1, 22.9, 22.8. ESI-MS: 338.2 $[M + H]^+$. HPLC retention time: 13.239 min. HPLC purity 97.7%.

5.1.20. *N*-(5-(5,6,7,8-tetrahydronaphthalen-2-yl)-1,3,4-oxadiazol-2-yl)-4-(chloro)benzamide (**15**).

Prepared using general procedure A with **4A** (0.050 g, 0.23 mmol, 1.0 eq.), 4-chlorobenzoyl chloride (0.049 g, 0.28 mmol, 1.2 eq.), and pyridine (1.0 mL) to produce **15** (0.047 g, 0.13 mmol, 57%) as a white solid. 1H NMR (500 MHz, DMSO- d_6): δ 8.07 (d, J = 8.1 Hz, 2H), 7.69 - 7.62 (m, 4H), 7.29 (d, J = 7.9 Hz, 1H), 2.81 (broad m, 4H), 1.77 (m, 4H). ^{13}C NMR (200 MHz, DMSO- d_6): δ 167.0, 165.3, 158.7, 141.6, 138.4, 138.1, 131.6, 130.8, 130.5, 129.9, 129.2, 126.9, 123.6, 29.3, 29.1, 22.8, 22.8. ESI-MS: 355.3 $[M + H]^+$. HPLC retention time: 13.573 min. HPLC purity 99.0%.

5.1.21. *N*-(5-(5,6,7,8-tetrahydronaphthalen-2-yl)-1,3,4-oxadiazol-2-yl)-4-(ethyl)benzamide (**16**).

Prepared using general procedure A with **4A** (0.050 g, 0.23 mmol, 1.0 eq.), 4-ethylbenzoyl chloride (0.039 g, 0.23 mmol, 1.0 eq.), and pyridine (1.0 mL) to produce **16** (0.032 g, 0.093 mmol, 40%) as a white solid. ¹H NMR (500 MHz, DMSO-*d*₆): δ 7.93 (m, 2H), 7.62 (m, 2H), 7.35 (d, *J* = 7.9 Hz, 2H), 7.24 (d, *J* = 8.0 Hz, 1H), 2.82-2.74 (m, 4H), 2.66 (q, *J* = 7.6 Hz, 2H), 1.74 – 1.71 (br m, 4H), 1.18 (t, *J* = 7.5 Hz, 3H). ¹³C NMR (126 MHz, DMSO-*d*₆): δ 160.9, 158.7, 149.1, 141.0, 138.0, 130.1, 128.6, 128.1, 126.5, 123.1, 120.8, 28.9, 28.7, 28.2, 22.5, 22.4, 15.3. APCI-MS: 348.3 [M + H]⁺. HPLC retention time: 13.633 min. HPLC purity 100%.

5.1.22. *N*-(5-(2,3-dihydrobenzo[*b*][1,4]dioxin-6-yl)-1,3,4-oxadiazol-2-yl)benzamide (**17**).

Prepared using general procedure A with **4B** (0.052 g, 0.24 mmol, 1.0 eq.), benzoyl chloride (0.037 g, 0.26 mmol, 1.1 eq.), and pyridine (1.0 mL) to produce **17** (0.032 g, 0.099 mmol, 42%) as a white solid. ¹H NMR (500 MHz, DMSO-*d*₆): δ 12.22 (s, 1H), 8.05 (d, *J* = 7.6 Hz, 2H), 7.63 (t, *J* = 7.4 Hz, 1H), 7.54 (t, *J* = 7.6 Hz, 2H), 7.44 (dd, *J* = 8.4, 2.1 Hz, 1H), 7.39 (d, *J* = 2.0 Hz, 1H), 7.08 (d, *J* = 8.4 Hz, 1H), 4.34 (q, *J* = 5.6 Hz, 4H). ¹³C NMR (200 MHz, DMSO-*d*₆): δ 146.3, 143.8, 132.3, 128.4, 128.3, 119.4, 118.1, 116.7, 114.5, 64.4, 64.1. ESI-MS: *m/z* 323.6 [M]⁺; HPLC retention time: 11.191 min. HPLC purity 99.6%.

5.1.23. *N*-(5-(2,3-dihydrobenzo[*b*][1,4]dioxin-6-yl)-1,3,4-oxadiazol-2-yl)-3-(thiomethoxy)benzamide (**18**).

Prepared using general procedure B with 3-thiomethoxybenzoic acid (0.025 g, 0.25 mmol, 1.1 eq.), oxalyl chloride (0.014 mL, 0.16 mmol, 1.2 eq.), **4B** (0.030 g, 0.14 mmol, 1.0 eq.), and pyridine (2.0 mL) to produce **18** (0.002 g, 0.005 mmol, 4%) as a white solid. ¹H NMR (800 MHz, DMSO-*d*₆): δ 7.90 (t, *J* = 1.8 Hz, 1H), 7.79 (d, *J* = 7.3 Hz, 1H), 7.50 – 7.39 (m, 3H), 7.36 (d, *J* = 2.0 Hz, 1H), 7.05 (d, *J* = 8.4 Hz, 1H), 4.35 – 4.29 (m, 4H), 2.54 (s, 3H). ¹³C NMR (200 MHz, DMSO-*d*₆): δ 163.2, 146.0, 143.8, 138.4, 128.9, 128.8, 125.3, 124.9, 119.2, 118.1, 117.2, 114.3, 64.4, 64.1, 40.0, 14.6. ESI-MS: *m/z* 339.7 [M + H]⁺, HPLC retention time: 11.946 min. HPLC purity 95.0%.

5.1.24. *N*-(5-(2,3-dihydrobenzo[*b*][1,4]dioxin-6-yl)-1,3,4-oxadiazol-2-yl)-3-(trifluoromethyl)benzamide (**19**).

Prepared using general procedure *B* with 3-trifluoromethylbenzoic acid (0.038 g, 0.20 mmol, 1.1 eq.), oxalyl chloride (0.018 mL, 0.21 mmol, 1.2 eq.), **4B** (0.040 g, 0.18 mmol, 1.0 eq.), and pyridine (2.0 mL) to produce **19** (0.013 g, 0.032 mmol, 18%) as a white solid. ^1H NMR (500 MHz, DMSO- d_6): δ 12.59 (s, 1H), 8.40 (s, 1H), 8.33 (d, J = 7.8 Hz, 1H), 8.03 (d, J = 7.8 Hz, 1H), 7.81 (t, J = 7.9 Hz, 1H), 7.45 (dd, J = 8.5, 2.1 Hz, 1H), 7.40 (t, J = 2.2 Hz, 1H), 7.09 (d, J = 8.5 Hz, 1H), 4.34 (q, J = 5.0 Hz, 4H). ^{13}C NMR (200 MHz, DMSO- d_6): δ 146.6, 143.9, 133.3, 132.5, 130.2, 130.0, 129.4 (q, J = 32.2 Hz), 125.0 (q, J = 4.0 Hz), 124.9, 123.9 (q, J = 271.4 Hz), 119.7, 118.3, 116.3, 114.7, 64.4, 64.2. ESI-MS: 391.6 $[\text{M}]^+$. HPLC retention time: 12.513 min. HPLC purity 99.1%.

5.1.25. *N*-(5-(2,3-dihydrobenzo[*b*][1,4]dioxin-6-yl)-1,3,4-oxadiazol-2-yl)-4-(isopropoxy)benzamide (**20**).

Prepared using general procedure *A* with **4B** (0.050 g, 0.23 mmol, 1.0 eq.), 4-isopropoxybenzoyl chloride (0.068 g, 0.34 mmol, 1.5 eq.), and pyridine (1.0 mL) to produce **20** (0.020 g, 0.052 mmol, 23%) as a white solid. ^1H NMR (500 MHz, DMSO- d_6): δ 12.00 (s, 1H), 8.01-7.99 (m, 2H), 7.44 – 7.35 (m, 2H), 7.08-7.01 (m, 3H), 4.77 – 4.72 (broad m, 1H), 4.36 – 4.32 (broad m, 4H), 1.30 (d, J = 6.0 Hz, 6H). ^{13}C NMR (126 MHz, CDCl_3): δ 160.9, 146.2, 143.9, 143.1, 130.5, 122.2, 119.4, 118.2, 116.9, 114.9, 114.5, 69.7, 64.4, 64.1, 21.8. ESI-MS: 382.1 $[\text{M} + \text{H}]^+$. HPLC retention time: 12.247 min. HPLC purity 100%.

5.1.26. *N*-(5-(2,3-dihydrobenzo[*b*][1,4]dioxin-6-yl)-1,3,4-oxadiazol-2-yl)-4-(bromo)benzamide (**21**).

Prepared using general procedure *B* with 4-bromobenzoic acid (0.053 g, 0.26 mmol, 1.1 eq.), oxalyl chloride (0.025 mL, 0.28 mmol, 1.2 eq.), **4B** (0.053 g, 0.26 mmol, 1.0 eq.), and pyridine (2.0 mL) to produce **21** (0.002 g, 0.005 mmol, 2%) as a white solid. ^1H NMR (800 MHz, DMSO- d_6): δ 12.27 (s, -1H), 7.97 (d, J = 8.1 Hz, 1H), 7.74 (d, J = 8.1 Hz, 2H), 7.42 (dd, J = 8.4, 2.1 Hz, 1H), 7.36 (d, J = 2.1 Hz, 1H), 7.06 (d, J = 8.4 Hz, 1H), 4.37 – 4.24 (m, 4H). ^{13}C NMR (200 MHz, DMSO- d_6): δ 146.8, 144.3, 132.0, 131.2, 130.9, 126.8, 119.9, 118.6, 117.0, 115.0, 64.9, 64.6. ESI-MS: m/z 401.8 $[\text{M}]^+$, 403.8 $[\text{M} + 2]^+$. HPLC retention time: 12.191 min. HPLC purity 96.7%.

5.1.27. *N*-(5-(2,3-dihydrobenzo[*b*][1,4]dioxin-6-yl)-1,3,4-oxadiazol-2-yl)-3-(methoxy)benzamide (**22**).

Prepared using general procedure *B* with 3-methoxybenzoic acid (0.034 g, 0.23 mmol, 1.1 eq.), oxalyl chloride (0.021 mL, 0.24 mmol, 1.2 eq.), **4B** (0.045 g, 0.21 mmol, 1.0 eq.), and pyridine (2.0 mL) to produce **22** (0.025 g, 0.071 mmol, 35%) as a white solid. ¹H NMR (500 MHz, DMSO-*d*₆): δ 12.36 (s, 1H), 7.69 – 7.64 (m, 2H), 7.46–7.38 (m, 2H), 7.18–7.09 (m, 2H), 6.62 (s, 1H), 4.41 – 4.34 (m, 4H), 3.86 (s, 3H). ¹³C NMR (200 MHz, DMSO-*d*₆): δ 169.9, 167.6, 162.1, 159.5, 146.4, 144.2, 136.1, 129.8, 121.2, 119.7, 118.6, 114.8, 113.6, 113.1, 110.5, 64.9, 64.6, 55.7. ESI-MS: 354.1 [M + H]⁺. HPLC retention time: 11.457 min. HPLC purity 95.6%.

5.1.28. *N*-(5-(2,3-dihydrobenzo[*b*][1,4]dioxin-6-yl)-1,3,4-oxadiazol-2-yl)-4-(methyl)benzamide (**23**).

Prepared using general procedure *A* with **4B** (0.040 g, 0.18 mmol, 1.0 eq.), 4-methylbenzoyl chloride (0.034 g, 0.22 mmol, 1.2 eq.), and pyridine (1.0 mL) to produce **23** (0.015 g, 0.044 mmol, 24%) as a white solid. ¹H NMR (500 MHz, DMSO-*d*₆): δ 12.02 (s, 1H), 7.97–7.90 (m, 2H), 7.84 – 7.76 (m, 1H), 7.45 (t, *J* = 8.3 Hz, 1H), 7.41 – 7.35 (m, 2H), 7.09 (t, *J* = 8.3 Hz, 1H), 4.34 (bs, 4H), 2.50 (s, 3H). ¹³C NMR (201 MHz, DMSO-*d*₆): δ 146.5, 143.9, 141.1, 131.5, 129.4, 129.2, 128.8, 128.4, 127.5, 119.7, 118.3, 116.4, 114.7, 64.5, 64.2, 21.1. ESI-MS: 337.9 [M]⁺. HPLC retention time: 11.666 min. HPLC purity 98.1%.

5.1.29. *N*-(5-(2,3-dihydrobenzo[*b*][1,4]dioxin-6-yl)-1,3,4-oxadiazol-2-yl)-3,4-(dimethyl)benzamide (**24**).

Prepared using general procedure *B* with 3,4-dimethylbenzoic acid (0.038 g, 0.25 mmol, 1.1 eq.), oxalyl chloride (0.023 mL, 0.26 mmol, 1.2 eq.), **4B** (0.050 g, 0.23 mmol, 1.0 eq.), and pyridine (2.0 mL) to produce **24** (0.030 g, 0.085 mmol, 37%) as a white solid. ¹H NMR (500 MHz, DMSO-*d*₆): δ 11.93 (s, 1H), 7.80 (s, 1H), 7.73 (d, *J* = 8.0 Hz, 1H), 7.40 (dd, *J* = 8.4, 2.1 Hz, 1H), 7.35 (bs, 1H), 7.27 (d, *J* = 7.9 Hz, 1H), 7.04 (d, *J* = 8.5 Hz), 4.30 (m, 4H), 2.27 (s, 3H), 2.05 (s, 3H). ¹³C NMR (200 MHz, DMSO-*d*₆): δ 146.8, 144.3, 137.0, 130.1, 129.8, 126.34, 120.0, 118.7, 117.1, 115.0, 64.9, 64.6, 20.0, 19.9. ESI-MS: 351.8 [M]⁺. HPLC retention time: 12.094 min. HPLC purity 100%.

5.1.30. *N*-(5-(thiophen-2-yl)-1,3,4-oxadiazol-2-yl)benzamide (**25**).

Prepared using general procedure *A* with **4C** (0.055 g, 0.33 mmol, 1.0 eq.), benzoyl chloride (0.051 g, 0.36 mmol, 1.1 eq.), and pyridine (2.0 mL) to produce **25** (0.055 g, 0.199 mmol, 60%) as a white solid. ¹H NMR (800 MHz, DMSO-*d*₆): δ 12.17 (s, 1H), 8.05 (d, *J* = 7.7 Hz, 2H), 7.94 (d, *J* = 4.9 Hz, 1H), 7.78 (d, *J* = 3.7 Hz,

1H), 7.67 (t, $J = 7.4$ Hz, 1H), 7.57 (t, $J = 7.6$ Hz, 2H), 7.30 (dd, $J = 5.0, 3.6$ Hz, 1H). ^{13}C NMR (200 MHz, DMSO- d_6): δ 165.0, 157.5, 157.4, 132.9, 132.2, 131.1, 129.7, 128.7, 128.6, 128.3, 124.3. ESI-MS: m/z 271.6 $[\text{M}]^+$; HPLC retention time: 10.957 min. HPLC purity 98.4%.

5.1.31. *N*-(5-(thiophen-2-yl)-1,3,4-oxadiazol-2-yl)-4-(bromo)benzamide (**26**).

Prepared using general procedure *B* with 4-bromobenzoic acid (0.071 g, 0.35 mmol, 1.1 eq.), oxalyl chloride (0.031 mL, 0.37 mmol, 1.2 eq.), **4C** (0.053 g, 0.22 mmol, 1.0 eq.), and pyridine (2.0 mL) to produce **26** (0.055 g, 0.199 mmol, 60%) as a white solid. ^1H NMR (800 MHz, DMSO- d_6): δ 12.23 (s, 1H), 7.98 – 7.91 (m, 3H), 7.80 – 7.74 (m, 3H), 7.28 (dd, 1H). ^{13}C NMR (200 MHz, DMSO- d_6): δ 164.55, 158.07, 157.58, 132.17, 131.65, 130.82, 130.16, 129.19, 127.39, 124.69. ESI-MS: m/z 349.9 $[\text{M}]^+$, 351.9 $[\text{M} + 2]^+$. HPLC retention time: 11.964 min. HPLC purity 97.6%.

5.1.32. *N*-(5-(thiophen-2-yl)-1,3,4-oxadiazol-2-yl)-3-(thiomethoxy)benzamide (**27**).

Prepared using general procedure *B* with 3-thiomethoxybenzoic acid (0.033 g, 0.20 mmol, 1.1 eq.), oxalyl chloride (0.019 mL, 0.22 mmol, 1.2 eq.), **4C** (0.030 g, 0.18 mmol, 1.0 eq.), and pyridine (2.0 mL) to produce **27** (0.006 g, 0.016 mmol, 12%) as a white solid. ^1H NMR (800 MHz, DMSO- d_6): δ 12.19 (s, 1H), 7.94 (dd, $J = 5.0, 1.2$ Hz, 1H), 7.87 (s, 1H), 7.79 – 7.76 (m, 2H), 7.54 (t, $J = 7.7$, 1H), 7.50 (t, $J = 7.7$ Hz, 1H), 7.30 (dd, $J = 5.0, 3.7$ Hz, 1H), 2.56 (s, 3H). ^{13}C NMR (200 MHz, DMSO- d_6): δ 164.5, 157.5, 157.2, 139.2, 132.9, 131.1, 130.0, 129.7, 129.2, 128.7, 124.9, 124.7, 124.3, 14.5. ESI-MS: m/z 317.7 $[\text{M}]^+$, 340.0 $[\text{M} + \text{Na}]^+$. HPLC retention time: 11.811 min. HPLC purity 97.3%.

5.1.33. *N*-(5-(thiophen-2-yl)-1,3,4-oxadiazol-2-yl)-4-(isopropoxy)benzamide (**28**).

Prepared using general procedure *A* with **4C** (0.049 g, 0.29 mmol, 1.0 eq.), 4-isopropoxybenzoyl chloride (0.064 g, 0.32 mmol, 1.1 eq.), and pyridine (2.0 mL) to produce **28** (0.058 g, 0.174 mmol, 59%) as a white solid. ^1H NMR (800 MHz, DMSO- d_6): δ 11.91 (br s, 1H), 7.99 (d, $J = 8.4$ Hz, 2H), 7.92 – 7.90 (m, 1H), 7.75 – 7.73 (m, 1H), 7.28 – 7.26 (m, 1H), 7.04 (d, $J = 8.5$ Hz, 2H), 4.74 (p, $J = 6.0$ Hz, 1H), 1.28 (d, $J = 6.1$ Hz, 6H). ^{13}C NMR (200 MHz, DMSO- d_6): δ 164.7, 161.8, 158.1, 157.9, 131.5, 131.0, 130.0, 129.1, 124.8, 124.1,

115.6, 70.1, 22.1. ESI-MS: m/z 330.1 $[M + H]^+$, 352.2 $[M + Na]^+$. HPLC retention time: 12.019 min. HPLC purity 98.7%.

5.1.34. *N*-(5-(thiophen-2-yl)-1,3,4-oxadiazol-2-yl)-4-(methoxy)benzamide (**29**).

Prepared using general procedure A with **4C** (0.029 g, 0.17 mmol, 1.0 eq.), 4-methoxybenzoyl chloride (0.033 g, 0.19 mmol, 1.1 eq.), and pyridine (2.0 mL) to produce **29** (0.014 g, 0.046 mmol, 27%) as a white solid. 1H NMR (800 MHz, DMSO- d_6): δ 11.94 (br s, 1H), 8.03 (d, J = 8.8 Hz, 2H), 7.93 (dd, J = 5.0, 1.2 Hz, 1H), 7.76 (dd, J = 3.6, 1.2 Hz, 1H), 7.29 (dd, J = 5.0, 3.7 Hz, 1H), 7.09 (d, J = 8.8 Hz, 2H), 3.86 (s, 3H). ^{13}C NMR (200 MHz, DMSO- d_6): δ 164.3, 163.0, 157.6, 131.1, 130.5, 129.6, 128.7, 124.4, 124.2, 113.9, 55.6, 39.5. ESI-MS: m/z 301.6 $[M + H]^+$. HPLC retention time: 11.009 min. HPLC purity 97.0%.

5.1.35. *N*-(5-(4-fluorophenyl)-1,3,4-oxadiazol-2-yl)benzamide (**30**).

Prepared using general procedure A with **4D** (0.025 g, 0.14 mmol, 1.0 eq.), benzoyl chloride (0.020 g, 0.14 mmol, 1.1 eq.), and pyridine (2.0 mL) to produce **30** (0.026 g, 0.091 mmol, 66%) as a pink solid. 1H NMR (800 MHz, DMSO- d_6): δ 12.17 (s, 1H), 8.08 – 8.00 (m, 4H), 7.68 (t, J = 7.4 Hz, 1H), 7.58 (t, J = 7.7 Hz, 2H), 7.47 (t, J = 8.8 Hz, 2H). ^{13}C NMR (200 MHz, DMSO- d_6): δ 165.0, 163.9 (d, J = 250.0 Hz) 160.5, 158.0, 132.9, 132.2, 128.7 (d, J = 9.2 Hz), 128.6, 128.3, 120.1, 116.7 (d, J = 22.4 Hz). ESI-MS: m/z 283.6 $[M]^+$, 306.0 $[M + Na]^+$. HPLC retention time: 11.428 min. HPLC purity 97.4%.

5.1.36. *N*-(5-(4-fluorophenyl)-1,3,4-oxadiazol-2-yl)-4-(bromo)benzamide (**31**).

Prepared using general procedure B with 4-bromobenzoic acid (0.036 g, 0.18 mmol, 1.1 eq.), oxalyl chloride (0.017 mL, 0.20 mmol, 1.2 eq.), **4D** (0.030 g, 0.17 mmol, 1.0 eq.), and pyridine (2.0 mL) to produce **31** (0.038 g, 0.17 mmol, 61%) as a pink solid. 1H NMR (800 MHz, DMSO- d_6): δ 12.28 (s, 1H), 8.06 – 8.01 (m, 2H), 7.98 (d, J = 8.1 Hz, 2H), 7.80 (d, J = 8.1 Hz, 2H), 7.50 – 7.44 (m, 2H). ^{13}C NMR (200 MHz, DMSO- d_6): δ 164.2, 164.0 (d, J = 249.7 Hz), 160.5, 157.8, 131.7, 131.4, 130.4, 128.8 (d, J = 9.1 Hz), 126.9, 120.0, 116.3 (d, J = 22.5 Hz). ESI-MS: m/z 361.9 $[M]^+$, 363.9 $[M + 2]^+$. HPLC retention time: 12.377 min. HPLC purity 97.1%.

5.1.37. *N*-(5-(4-fluorophenyl)-1,3,4-oxadiazol-2-yl)-3-(trifluoromethyl)benzamide (**32**).

Prepared using general procedure *B* with 3-trifluoromethylbenzoic acid (0.042 g, 0.24 mmol, 1.1 eq.), oxalyl chloride (0.022 mL, 0.26 mmol, 1.2 eq.), **4D** (0.040 g, 0.22 mmol, 1.0 eq.), and pyridine (2.0 mL) to produce **32** (0.022 g, 0.063 mmol, 28%) as a white solid. ¹H NMR (500 MHz, DMSO-*d*₆): δ 12.72 (s, 1H), 8.40 (s, 1H), 8.34 (d, *J* = 7.9 Hz, 1H), 8.06-8.00 (m, 3H), 7.80 (t, *J* = 7.8 Hz, 1H), 7.47 (t, *J* = 8.3 Hz, 2H). ¹³C NMR (126 MHz, DMSO-*d*₆): δ 164.7, 164.0 (d, *J* = 249.7 Hz), 159.8, 158.0, 132.5, 129.9, 128.8, 128.7, 128.6, 125.0, 123.9 (q, *J* = 271.4 Hz), 120.4, 116.8, 116.7. APCI-MS: *m/z* 352.2 [*M* + *H*]⁺. HPLC retention time: 12.643 min. HPLC purity 100%.

5.1.38. *N*-(5-(4-fluorophenyl)-1,3,4-oxadiazol-2-yl)-4-(methyl)benzamide (**33**).

Prepared using general procedure *A* with **4D** (0.023 g, 0.13 mmol, 1.0 eq.), 4-methylbenzoyl chloride (0.022 g, 0.14 mmol, 1.1 eq.), and pyridine (2.0 mL) to produce **33** (0.016 g, 0.054 mmol, 42%) as a white solid. ¹H NMR (500 MHz, DMSO-*d*₆): δ 12.10 (s, 1H), 8.05 – 8.02 (m, 2H), 7.96 (d, *J* = 7.9 Hz, 2H), 7.49 – 7.45 (m, 2H), 7.38 (d, *J* = 7.9 Hz, 2H), 2.41 (s, 3H). ¹³C NMR (126 MHz, DMSO-*d*₆): δ 164.9, 164.0 (q, *J* = 250.7 Hz), 160.5, 158.1, 143.4, 129.3, 128.8 (d, *J* = 10.1 Hz), 128.4, 120.1, 116.7 (d, *J* = 22.7 Hz), 21.1. ESI-MS: *m/z* 297.4 [*M*]⁺. HPLC retention time: 11.907 min. HPLC purity 99.3%.

5.1.39. *N*-(5-(4-fluorophenyl)-1,3,4-oxadiazol-2-yl)-3,4-(dimethyl)benzamide (**34**).

Prepared using general procedure *B* with 3,4-dimethylbenzoic acid (0.032 g, 0.21 mmol, 1.1 eq.), oxalyl chloride (0.020 mL, 0.22 mmol, 1.2 eq.), **4D** (0.035 g, 0.20 mmol, 1.0 eq.), and pyridine (2.0 mL) to produce **34** (0.015 g, 0.048 mmol, 25%) as a white solid. ¹H NMR (500 MHz, DMSO-*d*₆): δ 11.99 (s, 1H), 8.00 – 7.96 (m, 2H), 7.80 (bs, 1H), 7.74 (d, *J* = 7.8 Hz, 1H), 7.43 (t, *J* = 8.9 Hz, 2H), 7.29 (d, *J* = 7.9 Hz, 1H), 2.27 (s, 6H). ¹³C NMR (200 MHz, DMSO-*d*₆): δ 165.4, 164.4 (d, *J* = 248.0 Hz), 160.9, 158.5, 142.6, 137.2, 130.2, 130.1, 129.7, 129.2 (d, *J* = 10.0 Hz), 126.3, 120.6, 117.20 (d, *J* = 22.0 Hz), 20.0, 19.8. ESI-MS: *m/z* 311.5 [*M*]⁺. HPLC retention time: 12.304 min. HPLC purity 100%.

5.1.40. *N*-(5-(4-fluorophenyl)-1,3,4-oxadiazol-2-yl)-3-(methoxy)benzamide (**35**).

Prepared using general procedure *B* with 3-methoxybenzoic acid (0.023 g, 0.15 mmol, 1.1 eq.), oxalyl chloride (0.014 mL, 0.16 mmol, 1.2 eq.), **4D** (0.025 g, 0.214 mmol, 1.0 eq.), and pyridine (2.0 mL) to produce **35** (0.017 g, 0.054 mmol, 39%) as a white solid. ¹H NMR (500 MHz, DMSO-*d*₆): δ 12.27 (s, 1H), 8.02 (m, 2H), 7.70 – 7.53 (m, 2H), 7.46 (m, 3H), 7.20 (m, 1H), 3.84 (s, 3H). ¹³C NMR (200 MHz, DMSO-*d*₆): δ 166.3, 164.2 (d, *J* = 248.0 Hz), 160.4, 160.0, 159.6, 132.5, 130.1, 129.0 (d, *J* = 8.0 Hz), 121.1, 120.9, 118.9, 117.1 (d, *J* = 22.0 Hz), 113.6, 55.8. ESI-MS: *m/z* 313.8 [M]⁺. HPLC retention time: 11.669 min. HPLC purity 100%.

5.1.41. *N*-(5-(4-fluorophenyl)-1,3,4-oxadiazol-2-yl)-4-(methoxy)benzamide (**36**).

Prepared using general procedure *A* with **4D** (0.035 g, 0.20 mmol, 1.0 eq.), 4-methoxybenzoyl chloride (0.033 g, 0.20 mmol, 1.1 eq.), and pyridine (2.0 mL) to produce **36** (0.032 g, 0.10 mmol, 52%) as a white solid. ¹H NMR (500 MHz, DMSO-*d*₆): δ 12.01 (s, 1H), 8.04 (broad m, 4H), 7.47 (t, *J* = 8.7 Hz, 2H), 7.11 (broad m, 2H), 3.86 (s, 3H). ¹³C NMR (200 MHz, DMSO-*d*₆): δ 164.8, 164.4 (d, *J* = 248.0 Hz), 163.5, 161.0, 158.6, 131.0, 129.2 (d, *J* = 8.0 Hz), 124.6, 120.6, 117.2 (d, *J* = 22.0 Hz), 114.4, 56.1. ESI-MS: *m/z* 355.2 [M + CH₃CN + H]⁺. HPLC retention time: 11.533 min. HPLC purity 98.5%.

5.1.42. *N*-(5-(4-fluorophenyl)-1,3,4-oxadiazol-2-yl)-4-(piperidin-1-ylsulfonyl)benzamide (**37**).

Prepared using general procedure *B* with 3-(piperidin-1-sulfonyl)benzoic acid (0.080 g, 0.30 mmol, 1.0 eq.), oxalyl chloride (0.030 mL, 0.30 mmol, 1.2 eq.), **4D** (0.050 g, 0.30 mmol, 1.0 eq.), and pyridine (2.0 mL) to produce **37** (0.006 g, 0.014 mmol, 5%) as a white solid. ¹H NMR (500 MHz, DMSO-*d*₆): δ 8.35 (d, *J* = 2.0 Hz, 1H), 8.31 (d, *J* = 7.8 Hz, 1H), 8.01 – 7.88 (m, 4H), 7.76 (t, *J* = 7.8 Hz, 1H), 7.48 – 7.37 (m, 2H), 3.02 – 2.82 (m, 4H), 1.52 (m, *J* = 5.8 Hz, 4H), 1.33 (m, *J* = 8.1 Hz, 2H). ESI-MS: *m/z* 331.2 [M]⁺. HPLC retention time: 12.527 min. HPLC purity 96.1%.

5.1.43. *N*-(5-(4-fluorophenyl)-1,3,4-oxadiazol-2-yl)-3-(fluoro)benzamide (**38**).

Prepared using general procedure *A* with **4D** (0.033 g, 0.18 mmol, 1.0 eq.), 3-fluorobenzoyl chloride (0.031 g, 0.20 mmol, 1.1 eq.), and pyridine (2.0 mL) to produce **38** (0.033 g, 0.11 mmol, 62%) as a white solid. ¹H NMR (500 MHz, DMSO-*d*₆): δ 8.05-8.02 (broad m, 2H), 7.90 (d, *J* = 7.6 Hz, 1H), 7.85 (d, *J* = 9.8 Hz, 1H), 7.66-7.62 (broad m, 1H), 7.56-7.52 (broad m, 1H), 7.51-7.45 (broad m, 2H). ¹³C NMR (200 MHz, DMSO-*d*₆): δ

166.7, 164.5 (d, $J = 248.0$ Hz), 162.4 (d, $J = 244.0$ Hz), 160.8, 158.4, 135.2, 131.4, 129.3 (d, $J = 10.0$ Hz), 125.1, 120.4, 120.3, 117.2 (d, $J = 22.0$ Hz), 115.6 (d, $J = 24.0$ Hz). ESI-MS: m/z 365.1 $[M + CH_3CN + H]^+$. HPLC retention time: 11.823 min. HPLC purity 96.7%.

5.1.44. *N*-(5-(4-fluorophenyl)-1,3,4-oxadiazol-2-yl)-4-(fluoro)benzamide (39).

Prepared using general procedure A with **4D** (0.050 g, 0.28 mmol, 1.0 eq.), 4-fluorobenzoyl chloride (0.044 g, 0.28 mmol, 1.1 eq.), and pyridine (2.0 mL) to produce **39** (0.052 g, 0.17 mmol, 62%) as a white solid. 1H NMR (500 MHz, DMSO- d_6): δ 12.25 (s, 1H), 8.13 (broad m, 2H), 8.03 (broad m, 2H), 7.48 (t, $J = 8.6$ Hz, 2H), 7.42 (t, $J = 8.7$ Hz, 2H). ^{13}C NMR (200 MHz, DMSO- d_6): δ 165.3 (d, $J = 254.0$ Hz), 164.5 (d, $J = 248.0$ Hz), 164.3, 160.9, 158.4, 132.4, 131.7 (d, $J = 10.0$ Hz), 129.2 (d, $J = 10.0$ Hz), 120.5, 117.2 (d, $J = 22.0$ Hz), 116.2 (d, $J = 22.0$ Hz). APCI-MS: m/z 302.2 $[M + H]^+$. HPLC retention time: 11.695 min. HPLC purity 100%.

5.1.45. *N*-(5-(4-fluorophenyl)-1,3,4-oxadiazol-2-yl)-2-(fluoro)benzamide (40).

Prepared using general procedure B with 2-fluorobenzoic acid (0.034 g, 0.25 mmol, 1.1 eq.), oxalyl chloride (0.023 mL, 0.34 mmol, 1.2 eq.), **4D** (0.040 g, 0.22 mmol, 1.0 eq.), and pyridine (2.0 mL) to produce **40** (0.009 g, 0.031 mmol, 14%) as a white solid. 1H NMR (500 MHz, DMSO- d_6): δ 12.33 (s, 1H), 8.00-7.95 (m, 2H), 7.81-7.70 (m, 1H), 7.67-7.60 (m, 1H), 7.46-7.41 (m, 2H), 7.37-7.31 (m, 2H). ^{13}C NMR (200 MHz, DMSO- d_6): δ 165.5 (d, $J = 248.0$ Hz), 162.9, 161.8, 160.4, 158.5 (d, $J = 254.0$ Hz), 134.5 (d, $J = 8.0$ Hz), 130.8, 129.3 (d, $J = 8.0$ Hz), 126.3, 125.2, 120.4, 117.2 (d, $J = 22.0$ Hz), 116.9 (d, $J = 20.0$ Hz). ESI-MS: m/z 302.2 $[M + H]^+$. HPLC retention time: 11.474 min. HPLC purity 99.5%.

5.1.46. *N*-(5-(4-fluorophenyl)-1,3,4-oxadiazol-2-yl)-4-(ethyl)benzamide (41).

Prepared using general procedure A with **4D** (0.050 g, 0.28 mmol, 1.0 eq.), 4-ethylbenzoyl chloride (0.047 g, 0.28 mmol, 1.1 eq.), and pyridine (2.0 mL) to produce **41** (0.048 g, 0.15 mmol, 55%) as a white solid. 1H NMR (800 MHz, DMSO- d_6): δ 12.06 (s, 1H), 8.04 – 8.02 (m, 2H), 7.97 (d, $J = 7.8$ Hz, 2H), 7.48 – 7.45 (m, 2H), 7.41 (d, $J = 7.8$ Hz, 2H), 2.71 (q, $J = 7.6$ Hz, 2H), 1.22 (t, $J = 7.6$ Hz, 3H). ^{13}C NMR (200 MHz, DMSO- d_6): δ 164.7, 163.8 (d, $J = 250.0$ Hz), 160.4, 157.9, 149.3, 129.5, 128.7 (d, $J = 8.0$ Hz), 128.4, 128.0, 120.0, 116.6 (d, $J = 22.0$ Hz), 28.0, 15.1. APCI-MS: m/z 312.2 $[M+H]^+$. HPLC retention time: 12.433 min. HPLC purity 100%.

5.1.47. *N*-(5-(4-fluorophenyl)-1,3,4-oxadiazol-2-yl)-4-(chloro)benzamide (**42**).

Prepared using general procedure A with **4D** (0.050 g, 0.28 mmol, 1.0 eq.), 4-chlorobenzoyl chloride (0.049 g, 0.28 mmol, 1.1 eq.), and pyridine (2.0 mL) to produce **42** (0.043 g, 0.14 mmol, 48%) as a white solid. ¹H NMR (500 MHz, DMSO-*d*₆): δ 12.31 (s, 1H), 8.07 – 8.02 (m, 4H), 7.73-7.62 (m, 2H), 7.47 (t, *J* = 8.7 Hz, 2H). ¹³C NMR (126 MHz, DMSO-*d*₆): δ 164.1 (d, *J* = 250.7 Hz), 164.0, 160.5, 157.9, 132.3, 131.20, 130.3, 129.6, 128.8 (d, *J* = 9.1 Hz), 120.1, 116.8 (d, *J* = 22.7 Hz). APCI-MS: *m/z* 318.1 [M + H]⁺. HPLC retention time: 12.269 min. HPLC purity 99.1%.

5.1.48. *N*-(5-(4-fluorophenyl)-1,3,4-oxadiazol-2-yl)-4-(phenyl)benzamide (**43**).

Prepared using general procedure A with **4D** (0.050 g, 0.28 mmol, 1.0 eq.), 4-phenylbenzoyl chloride (0.073 g, 0.33 mmol, 1.1 eq.), and pyridine (2.0 mL) to produce **43** (0.045 g, 0.13 mmol, 45%) as a white solid. ¹H NMR (500 MHz, DMSO-*d*₆): δ 12.31 (s, 1H), 8.13 (d, *J* = 8.1 Hz, 2H), 8.03-7.99 (m, 2H), 7.85 (d, *J* = 8.1 Hz, 2H), 7.76 (d, *J* = 7.8 Hz, 2H), 7.51 – 7.40 (m, 5H). ¹³C NMR (126 MHz, DMSO-*d*₆): δ 164.2 (d, *J* = 249.4 Hz), 163.5, 160.3, 160.2, 144.5, 139.2, 134.5, 130.3, 129.4, 129.0 (d, *J* = 8.8 Hz), 128.7, 127.3, 127.1, 120.6, 117.1 (d, *J* = 22.6 Hz). APCI-MS: *m/z* 360.2 [M + H]⁺. HPLC retention time: 12.916 min. HPLC purity 96.1%.

5.1.50. *N*-(5-(4-fluorophenyl)-1,3,4-oxadiazol-2-yl)-3-(phenyl)benzamide (**44**).

Prepared using general procedure A with **4D** (0.050 g, 0.28 mmol, 1.0 eq.), 3-phenylbenzoyl chloride (0.060 g, 0.28 mmol, 1.1 eq.), and pyridine (2.0 mL) to produce **44** (0.043 g, 0.120 mmol, 43%) as a white solid. ¹H NMR (500 MHz, DMSO-*d*₆): δ 12.36 (s, 1H), 8.38 (s, 1H), 8.08 – 7.99 (m, 4H), 7.83 (d, *J* = 7.7 Hz, 2H), 7.69 (t, *J* = 7.8 Hz, 1H), 7.51 – 7.44 (t, *J* = 7.6 Hz, 2H), 7.47 (m, 3H). ¹³C NMR (200 MHz, DMSO-*d*₆): δ 165.25, 164.44 (d, *J* = 248.0 Hz), 160.88, 158.47, 140.96, 139.59, 133.27, 131.55, 129.96, 129.54, 129.24 (d, *J* = 10.0 Hz), 128.50, 127.92, 127.38, 126.86, 120.51, 117.21 (d, *J* = 22.0 Hz). APCI-MS: *m/z* 360.2 [M + H]⁺. HPLC retention time: 13.009 min. HPLC purity 100%.

5.1.49. *N*-(5-cyclohexyl-1,3,4-oxadiazol-2-yl)benzamide (**45**).

Prepared using general procedure A with **4E** (0.053 g, 0.32 mmol, 1.0 eq.), benzoyl chloride (0.049 g, 0.35 mmol, 1.1 eq.), and pyridine (2.0 mL) to produce **45** (0.035 g, 0.125 mmol, 40%) as a white solid. ¹H NMR

(800 MHz, DMSO- d_6): δ 11.87 (br s, 1H), 8.01 (d, J = 7.6 Hz, 2H), 7.65 (t, J = 7.4 Hz, 1H), 7.55 (t, J = 7.6 Hz, 2H), 2.98 – 2.91 (m, 1H), 2.04 – 1.99 (m, 2H), 1.75 (dt, J = 13.4, 4.0 Hz, 2H), 1.65 (dt, J = 13.0, 4.0 Hz, 1H), 1.54 (qd, J = 11.6, 3.5 Hz, 2H), 1.39 (qt, J = 11.9, 3.6 Hz, 2H), 1.28 (qt, J = 11.9, 3.6 Hz, 1H). ^{13}C NMR (200 MHz, DMSO- d_6): δ 166.8, 165.1, 157.5, 132.8, 132.3, 128.6, 128.2, 34.2, 29.4, 25.2, 24.6. ESI-MS: m/z 271.7 $[\text{M}]^+$; HPLC retention time: 11.721 min. HPLC purity 95.1%.

5.1.50. *N*-(5-cyclohexyl-1,3,4-oxadiazol-2-yl)-4-(bromo)benzamide (**46**).

Prepared using general procedure *B* with 4-bromobenzoic acid (0.033 g, 0.16 mmol, 1.1 eq.), oxalyl chloride (0.016 mL, 0.18 mmol, 1.2 eq.), **4E** (0.025 g, 0.15 mmol, 1.0 eq.), and pyridine (2.0 mL) to produce **46** (0.041 g, 0.12 mmol, 77%) as a white solid. ^1H NMR (500 MHz, DMSO- d_6): δ 12.06 – 11.91 (m, 1H), 7.93 (d, J = 8.0 Hz, 2H), 7.80 (d, J = 8.0 Hz, 2H), 2.95 (s, 1H), 2.01 (dt, J = 13.3, 3.9 Hz, 2H), 1.75 (dp, J = 11.9, 3.9 Hz, 2H), 1.65 (dt, J = 12.8, 4.0 Hz, 1H), 1.59 – 1.49 (m, 2H), 1.40 (qt, J = 11.9, 3.4 Hz, 2H), 1.28 (m, 1H). ^{13}C NMR (200 MHz, DMSO- d_6): δ 167.4, 164.6, 157.7, 150.0, 132.1, 130.7, 127.3, 34.6, 29.9, 25.6, 25.0. ESI-MS: m/z 349.9 $[\text{M}]^+$, 351.9 $[\text{M} + 2]^+$; HPLC retention time: 12.760 min. HPLC purity 98%.

5.1.51. *N*-(5-cyclohexyl-1,3,4-oxadiazol-2-yl)-3-(thiomethoxy)benzamide (**47**).

Prepared using general procedure *B* with 3-thiomethoxybenzoic acid (0.033 g, 0.20 mmol, 1.1 eq.), oxalyl chloride (0.019 mL, 0.22 mmol, 1.2 eq.), **4E** (0.030 g, 0.18 mmol, 1.0 eq.), and pyridine (2.0 mL) to produce **47** (0.013 g, 0.040 mmol, 23%) as a white solid. ^1H NMR (800 MHz, DMSO- d_6): δ 11.91 (s, 1H), 7.84 (s, 1H), 7.75 – 7.72 (m, 1H), 7.54 – 7.50 (m, 1H), 7.47 (t, J = 7.8 Hz, 1H), 2.94 (tt, J = 11.1, 3.9 Hz, 1H), 2.55 (s, 3H), 2.02 – 1.96 (m, 2H), 1.74 (dt, J = 13.3, 4.0 Hz, 2H), 1.65 (dt, J = 12.9, 4.0 Hz, 1H), 1.57 – 1.50 (m, 2H), 1.43 – 1.33 (m, 2H), 1.31 – 1.23 (m, 1H). ^{13}C NMR (200 MHz, DMSO- d_6): δ 167.3, 165.1, 157.9, 139.6, 133.5, 130.4, 129.6, 125.4, 125.1, 34.6, 29.9, 25.6, 25.1, 15.0. ESI-MS: m/z 317.7 $[\text{M}]^+$; HPLC retention time: 12.531 min. HPLC purity 96.9%.

5.1.52. *N*-(5-cyclohexyl-1,3,4-oxadiazol-2-yl)-3-(trifluoromethyl)benzamide (**48**).

Prepared using general procedure *B* with 3-trifluoromethylbenzoic acid (0.050 g, 0.26 mmol, 1.1 eq.), oxalyl chloride (0.024 mL, 0.28 mmol, 1.2 eq.), **4E** (0.040 g, 0.24 mmol, 1.0 eq.), and pyridine (2.0 mL) to

produce **48** (0.035 g, 0.10 mmol, 43%) as a white solid. ^1H NMR (500 MHz, $\text{DMSO}-d_6$): δ 12.52 (s, 1H), 8.36 (s, 1H), 8.31 (d, $J = 7.9$ Hz, 1H), 8.01 (d, $J = 7.8$ Hz, 1H), 7.79 (t, $J = 8.0$ Hz, 1H), 2.94 (m, 1H), 2.01 (m, 2H), 1.75 (m, 2H), 1.69 – 1.62 (m, 1H), 1.53 (m, 2H), 1.43 – 1.36 (m, 2H), 1.32 – 1.23 (m, 1H). ^{13}C NMR (200 MHz, $\text{DMSO}-d_6$): δ 165.5, 165.2, 157.7, 135.6, 132.7, 131.9, 129.4, 128.7 (q, $J = 32.0$ Hz), 124.4, 123.3 (q, $J = 270.0$ Hz), 33.6, 28.8, 24.6, 24.0. ESI-MS: m/z 339.5 $[\text{M}]^+$. HPLC retention time: 13.035 min. HPLC purity 95.6%.

5.1.53. *N*-(5-cyclohexyl-1,3,4-oxadiazol-2-yl)-3,4-(dimethyl)benzamide (**49**).

Prepared using general procedure *B* with 3,4-dimethylbenzoic acid (0.043 g, 0.26 mmol, 1.1 eq.), oxalyl chloride (0.023 mL, 0.28 mmol, 1.2 eq.), **4E** (0.040 g, 0.24 mmol, 1.0 eq.), and pyridine (2.0 mL) to produce **49** (0.018 g, 0.060 mmol, 25%). ^1H NMR (500 MHz, CDCl_3): δ 11.30 (s, 1H), 7.87 (s, 1H), 7.81 (d, $J = 8.0$ Hz, 1H), 7.18 (d, $J = 7.2$ Hz, 1H), 2.85 (broad s, 1H), 2.27 (s, 6H), 2.09–2.04 (m, 2H), 1.81–1.77 (m, 2H), 1.68–1.65 (m, 1H), 1.61 – 1.56 (m, 2H), 1.38 – 1.32 (m, 2H), 1.31 – 1.24 (m, 1H). ESI-MS: m/z 299.6 $[\text{M}]^+$. HPLC retention time: 13.038 min. HPLC purity 96%.

5.1.54. *N*-(5-cyclohexyl-1,3,4-oxadiazol-2-yl)-4-(isopropoxy)benzamide (**50**).

Prepared using general procedure *A* with **4E** (0.049 g, 0.29 mmol, 1.0 eq.), 4-isopropoxybenzoyl chloride (0.064 g, 0.32 mmol, 1.1 eq.), and pyridine (2.0 mL) to produce **50** (0.018 g, 0.051 mmol, 18%) as a white solid. ^1H NMR (800 MHz, $\text{DMSO}-d_6$): δ 11.63 (s, 1H), 7.96 – 7.93 (m, 2H), 7.03 – 7.00 (m, 2H), 4.73 (hept, $J = 6.0$ Hz, 1H), 2.93 – 2.89 (m, 1H), 2.00 – 1.96 (m, 2H), 1.75 – 1.70 (m, 2H), 1.65 – 1.60 (m, 1H), 1.55 – 1.48 (m, 2H), 1.40 – 1.34 (m, 2H), 1.28 (d, $J = 5.9$ Hz, 6H), 1.27 – 1.22 (m, 1H). ^{13}C NMR (201 MHz, $\text{DMSO}-d_6$): δ 167.0, 165.1 (d, $J = 43.9$ Hz), 161.6, 158.3, 130.9, 124.6, 115.5, 70.1, 34.6, 29.9, 25.6, 25.1, 22.1. ESI-MS: m/z 329.7 $[\text{M}]^+$. HPLC retention time: 12.672 min. HPLC purity 95.1%.

5.1.55. *N*-(5-cyclohexyl-1,3,4-oxadiazol-2-yl)-4-(methoxy)benzamide (**51**).

Prepared using general procedure *A* with **4E** (0.032 g, 0.19 mmol, 1.0 eq.), 4-methoxybenzoyl chloride (0.033 g, 0.19 mmol, 1.1 eq.), and pyridine (2.0 mL) to produce **51** (0.022 g, 0.073 mmol, 38%) as a white solid. ^1H NMR (500 MHz, $\text{DMSO}-d_6$): δ 11.73 (s, 1H), 8.02 (d, $J = 8.5$ Hz, 2H), 7.10 (d, $J = 8.6$ Hz, 2H), 3.87 (s, 3H), 2.96 (broad m, 1H), 2.04 – 1.99 (broad m, 1H), 1.78 – 1.76 (broad m, 2H), 1.69 – 1.66 (broad m, 1H),

1.59-1.50 (m, 2H), 1.45-1.38 (m, 2H), 1.33 – 1.16 (m, 2H). ^{13}C NMR (126 MHz, $\text{DMSO}-d_6$): δ 166.9, 164.4, 162.9, 157.6, 130.4, 124.2, 113.9, 55.6, 34.2, 29.5, 25.2, 24.7. ESI-MS: m/z 300.0 $[\text{M}-\text{H}]^-$. HPLC retention time: 11.795 min. HPLC purity 95.2%.

5.1.56. *N*-(5-cyclohexyl-1,3,4-oxadiazol-2-yl)-4-(methyl)benzamide (52).

Prepared using general procedure A with **4E** (0.050 g, 0.30 mmol, 1.0 eq.), 4-methylbenzoyl chloride (0.051 g, 0.33 mmol, 1.1 eq.), and pyridine (2.0 mL) to produce **52** (0.042 g, 0.15 mmol, 49%) as a white solid. ^1H NMR (500 MHz, $\text{DMSO}-d_6$): δ 11.79 (s, 1H), 7.91 (broad d, $J = 8.4$ Hz, 2H), 7.35 (broad d, $J = 7.9$ Hz), 2.99 – 2.91 (m, 1H), 2.39 (s, 3H), 2.05-1.98 (m, 2H), 1.77 – 1.72 (m, 2H), 1.67 – 1.63 (m, 1H), 1.58 – 1.49 (m, 2H), 1.43 – 1.35 (m, 2H), 1.31 – 1.23 (m, 1H). ^{13}C NMR (200 MHz, $\text{DMSO}-d_6$): δ 166.8, 164.8, 157.4, 143.1, 129.3, 129.1, 128.2, 34.1, 29.3, 25.1, 24.5, 21.0. ESI-MS: m/z 285.6 $[\text{M}]^+$. HPLC retention time: 12.163 min. HPLC purity 100%.

5.1.57. *N*-(5-cyclohexyl-1,3,4-oxadiazol-2-yl)-4-(ethyl)benzamide (53).

Prepared using general procedure A with **4E** (0.038 g, 0.23 mmol, 1.0 eq.), 4-ethylbenzoyl chloride (0.038 g, 0.23 mmol, 1.1 eq.), and pyridine (2.0 mL) to produce **53** (0.020 g, 0.066 mmol, 29%) as a white solid. ^1H NMR (500 MHz, $\text{DMSO}-d_6$): δ 11.89 (s, 1H), 7.93 (d, $J = 8.0$ Hz, 2H), 7.38 (d, $J = 8.0$ Hz, 2H), 2.96-2.90 (broad m, 1H), 2.69 (q, $J = 7.7$ Hz, 2H), 2.02 – 1.98 (broad m, 2H), 1.77 – 1.73 (broad m, 2H), 1.67 – 1.63 (broad m, 1H), 1.57 – 1.49 (m, 2H), 1.43-1.35 (m, 2H), 1.31 – 1.26 (broad m, 1H), 1.21 (t, $J = 7.6$ Hz, 3H). ^{13}C NMR (200 MHz, $\text{DMSO}-d_6$): δ 167.0, 165.9, 158.5, 149.5, 130.7, 128.9, 128.4, 34.6, 29.9, 28.6, 25.6, 25.1, 15.7. ESI-MS: m/z 300.2 $[\text{M} + \text{H}]^+$. HPLC retention time: 12.732 min. HPLC purity 95.5%.

5.1.58. *N*-(5-cyclohexyl-1,3,4-oxadiazol-2-yl)-4-(fluoro)benzamide (54).

Prepared using general procedure A with **4E** (0.035 g, 0.21 mmol, 1.0 eq.), 4-fluorobenzoyl chloride (0.033 g, 0.21 mmol, 1.1 eq.), and pyridine (2.0 mL) to produce **54** (0.026 g, 0.090 mmol, 43%) as a white solid. ^1H NMR (500 MHz, $\text{DMSO}-d_6$): δ 12.13 (s, 1H), 8.15 – 8.04 (m, 2H), 7.42-7.34 (m, 2H), 2.98 – 2.93 (broad m, 1H), 2.04-1.99 (broad m, 2H), 1.78 – 1.73 (broad m, 2H), 1.67 – 1.64 (broad m, 1H), 1.561-1.51 (m, 2H), 1.44- 1.36 (m, 2H), 1.31-1.24 (m, 1H). ^{13}C NMR (200 MHz, $\text{DMSO}-d_6$): δ 168.4, 167.3, 165.2 (d, $J = 246.0$

Hz), 153.6, 131.7 (d, $J = 10.0$ Hz), 127.5, 116.1 (d, $J = 22.0$ Hz), 34.6, 29.9, 25.6, 25.1. ESI-MS: m/z 290.1 $[M + H]^+$. HPLC retention time: 12.251 min. HPLC purity 98.9%.

5.1.59. *N*-(5-cyclohexyl-1,3,4-oxadiazol-2-yl)-3-(fluoro)benzamide (**55**).

Prepared using general procedure A with **4E** (0.040 g, 0.24 mmol, 1.0 eq.), 3-fluorobenzoyl chloride (0.038 g, 0.24 mmol, 1.1 eq.), and pyridine (2.0 mL) to produce **55** (0.034 g, 0.12 mmol, 49%) as a white solid. ^1H NMR (500 MHz, DMSO- d_6): δ 12.04 (s, 1H), 7.86 (d, $J = 7.8$ Hz, 1H), 7.81 – 7.79 (m, 1H), 7.65–7.57 (m, 1H), 7.51 (t, $J = 8.6$ Hz, 1H), 2.96 – 2.92 (broad m, 1H), 2.02 – 1.99 (broad m, 2H), 1.77–1.72 (broad m, 2H), 1.67–1.63 (broad m, 1H), 1.57 – 1.49 (m, 2H), 1.43 – 1.35 (m, 2H), 1.31–1.23 (m, 1H). ^{13}C NMR (126 MHz, DMSO- d_6): δ 162.0 (d, $J = 252.0$ Hz), 130.9 (d, $J = 8.9$ Hz), 124.6, 119.7 (d, $J = 21.4$ Hz), 115.1 (d, $J = 22.7$ Hz), 34.2, 29.4, 25.2, 24.6. APCI-MS: m/z 290.2 $[M + H]^+$. HPLC retention time: 12.425 min. HPLC purity 98.3%.

5.1.60. *N*-(5-cyclohexyl-1,3,4-oxadiazol-2-yl)-4-(chloro)benzamide (**56**).

Prepared using general procedure A with **4E** (0.040 g, 0.24 mmol, 1.0 eq.), 4-chlorobenzoyl chloride (0.042 g, 0.24 mmol, 1.0 eq.), and pyridine (2.0 mL) to produce **56** (0.030 g, 0.098 mmol, 41%) as a white solid. ^1H NMR (800 MHz, DMSO- d_6): δ 11.98 (m, 1H), 8.02 (d, $J = 8.2$ Hz, 2H), 7.62 (d, $J = 8.2$ Hz, 2H), 2.94 – 2.92 (m, 1H), 2.01 – 2.00 (m, 2H), 1.76 – 1.73 (m, 2H), 1.65 – 1.64 (m, 1H), 1.56 – 1.51 (m, 2H), 1.41 – 1.37 (m, 2H), 1.29 – 1.25 (m, 1H). ^{13}C NMR (200 MHz, DMSO- d_6): δ 167.3, 164.5, 157.9, 138.1, 130.7, 129.2, 34.6, 29.8, 25.6, 25.1. ESI-MS: m/z 306.2 $[M + H]^+$. HPLC retention time: 12.639 min. HPLC purity 98.0%.

5.1.61. *N*-(5-cyclohexyl-1,3,4-oxadiazol-2-yl)-3-(phenyl)benzamide (**57**).

Prepared using general procedure A with **4E** (0.050 g, 0.30 mmol, 1.0 eq.), 3-phenylbenzoyl chloride (0.065 g, 0.30 mmol, 1.0 eq.), and pyridine (2.0 mL) to produce **57** (0.032 g, 0.092 mmol, 31%) as a white solid. ^1H NMR (500 MHz, DMSO- d_6): δ 12.06 (s, 1H), 8.33 (m, 1H), 7.99 (m, 2H), 7.80 (m, 2H), 7.66 (m, 1H), 7.54 (m, 2H), 7.44 (q, $J = 6.8$ Hz, 1H), 2.99 – 2.94 (m, 1H), 2.04 – 2.02 (m, 2H), 1.78 – 1.76 (m, 2H), 1.68 – 1.65 (m, 1H), 1.60 – 1.52 (m, 2H), 1.45 – 1.37 (m, 2H), 1.32 – 1.25 (m, 1H). ^{13}C NMR (126 MHz, DMSO- d_6): δ

166.8, 164.9, 157.5, 140.5, 139.2, 133.0, 131.0, 129.5, 129.1, 128.1, 127.5, 127.0, 126.4, 34.2, 29.5, 25.2, 24.7. APCI-MS: m/z 348.3 $[M + H]^+$. HPLC retention time: 13.318 min. HPLC purity 99.2%.

5.1.62. *N*-(5-(5,6,7,8-tetrahydronaphthalen-2-yl)-1,3,4-oxadiazol-2-yl)-3-(methyl)-5-(trifluoromethyl)benzamide (58).

Prepared using general procedure A with **4A** (0.030 g, 0.14 mmol, 1.0 eq.), 3-methyl-5-(trifluoromethyl)benzoyl chloride (0.031 g, 0.14 mmol, 1.0 eq.), and pyridine (2.0 mL) to produce **58** (0.018 g, 0.045 mmol, 32%) as a white solid. ^1H NMR (500 MHz, $\text{DMSO}-d_6$): δ 12.44 (s, 1H), 8.19 – 8.16 (broad m, 2H), 7.87 (s, 1H), 7.68 – 7.66 (m, 2H), 7.29 (d, $J = 7.9$ Hz, 1H), 2.85 – 2.80 (m, 4H), 2.50 (s, 3H), 1.79 – 1.76 (m, 4H). ^{13}C NMR (201 MHz, $\text{DMSO}-d_6$) δ 141.2, 140.1, 138.0, 132.9, 130.1, 129.7, 129.3 (q, $J = 32.2$ Hz), 126.5, 123.9 (q, $J = 270.0$ Hz), 123.1, 122.2, 120.5, 28.9, 28.6, 22.4, 22.3, 20.7. APCI-MS: m/z 402.2 $[M + H]^+$. HPLC retention time: 12.963 min. HPLC purity 100%.

5.1.63. *N*-(5-(5,6,7,8-tetrahydronaphthalen-2-yl)-1,3,4-oxadiazol-2-yl)-4-(methyl)-3-(trifluoromethyl)benzamide (59).

Prepared using general procedure A with **4A** (0.050 g, 0.23 mmol, 1.0 eq.), 4-methyl-3-(trifluoromethyl)benzoyl chloride (0.052 g, 0.23 mmol, 1.0 eq.), and pyridine (2.0 mL) to produce **59** (0.056 g, 0.14 mmol, 60%). ^1H NMR (500 MHz, $\text{DMSO}-d_6$): δ 12.55 (s, 1H), 8.35 (s, 1H), 8.22 (d, $J = 8.1$ Hz, 1H), 7.68 – 7.65 (m, 3H), 7.28 (d, $J = 7.9$ Hz, 1H), 2.83 – 2.75 (m, 4H), 2.51 (s, 3H), 1.78 – 1.76 (m, 4H). ^{13}C NMR (126 MHz, $\text{DMSO}-d_6$): δ 141.26, 141.16, 137.95, 132.76, 132.25, 130.08, 127.75, 127.51, 126.50, 125.67, 123.11, 120.48, 28.89, 28.63, 22.39, 22.34, 18.93. APCI-MS: m/z 402.2 $[M + H]^+$. HPLC retention time: 14.099 min. HPLC purity 97.1%.

5.1.64. *N*-(5-(5,6,7,8-tetrahydronaphthalen-2-yl)-1,3,4-oxadiazol-2-yl)-3-(methoxy)-5-(trifluoromethyl)benzamide (60).

Prepared using general procedure A with **4A** (0.050 g, 0.23 mmol, 1.0 eq.), 3-methoxy-5-(trifluoromethyl) benzoyl chloride (0.067 g, 0.28 mmol, 1.0 eq.), and pyridine (2.0 mL) to produce **60** (0.041 g, 0.098 mmol, 42%) as a white solid. ^1H NMR (500 MHz, $\text{DMSO}-d_6$): δ 12.53 (s, 1H), 7.96 (s, 1H), 7.87 (s, 1H),

7.68 – 7.65 (m, 2H), 7.54 (s, 1H), 7.28 (d, $J = 8.0$ Hz, 1H), 3.94 (s, 3H), 2.84 – 2.80 (m, 4H), 1.78 – 1.76 (m, 4H). ^{13}C NMR (200 MHz, DMSO- d_6): δ 167.8, 161.5, 160.3, 158.1, 141.7, 138.4, 135.4, 131.1 (q, $J = 32.0$ Hz), 130.5, 127.0, 124.1 (q, $J = 270.0$ Hz), 123.6, 120.9, 118.1, 117.4, 115.5, 56.6, 29.3, 29.1, 22.8, 22.8. APCI-MS: m/z 418.2 $[\text{M} + \text{H}]^+$. HPLC retention time: 14.048 min. HPLC purity 100%.

5.1.65. *N*-(5-(4-fluorophenyl)-1,3,4-oxadiazol-2-yl)-3-(methyl)-5-(trifluoromethyl)benzamide (**61**).

Prepared using general procedure A with **4D** (0.032 g, 0.18 mmol, 1.0 eq.), 3-methyl-5-(trifluoromethyl)benzoyl chloride (0.048 g, 0.21 mmol, 1.1 eq.), and pyridine (2.0 mL) to produce **61** (0.026 g, 0.071 mmol, 40%) as a white solid. ^1H NMR (500 MHz, DMSO- d_6): δ 12.46 (s, 1H), 8.24-8.16 (broad m, 2H), 8.06-8.02 (broad m, 2H), 7.88 (s, 1H), 7.56 – 7.44 (broad m, 2H), 2.50 (s, 3H). ^{13}C NMR (200 MHz, DMSO- d_6): δ 166.1, 164.5 (d, $J = 248.0$ Hz), 160.8, 158.5, 140.5, 133.7, 133.4, 130.1, 129.8 (q, $J = 32.0$ Hz), 129.3 (d, $J = 8.0$ Hz), 124.4 (q, $J = 270.0$ Hz), 122.6, 120.5, 117.2 (d, $J = 22.0$ Hz), 21.1. ESI-MS: m/z 366.1 $[\text{M} + \text{H}]^+$. HPLC retention time: 13.050 min. HPLC purity 100%.

5.1.66. *N*-(5-(4-fluorophenyl)-1,3,4-oxadiazol-2-yl)-4-(methyl)-3-(trifluoromethyl)benzamide (**62**).

Prepared using general procedure A with **4D** (0.050 g, 0.28 mmol, 1.0 eq.), 4-methyl-3-(trifluoromethyl)benzoyl chloride (0.075 g, 0.33 mmol, 1.2 eq.), and pyridine (2.0 mL) to produce **62** (0.039 g, 0.11 mmol, 38%). ^1H NMR (500 MHz, DMSO- d_6): δ 12.48 (s, 1H), 8.35 (s, 1H), 8.22 (d, $J = 8.0$ Hz, 1H), 8.04 – 8.02 (m, 2H), 7.66 (d, $J = 8.0$ Hz, 1H), 7.47 (t, $J = 8.5$ Hz, 2H), 2.51 (s, 3H). ^{13}C NMR (200 MHz, DMSO- d_6): δ 164.5 (d, $J = 248.0$ Hz), 164.2, 160.5, 158.6, 141.8, 133.2, 132.7, 131.1, 129.2 (d, $J = 10.0$ Hz), 128.1 (q, $J = 28.0$ Hz), 126.1, 124.6 (q, $J = 272.0$ Hz), 120.5, 117.2 (d, $J = 22.0$ Hz), 19.4. APCI-MS: m/z 366.2 $[\text{M} + \text{H}]^+$. HPLC retention time: 12.974 min. HPLC purity 96.4%.

5.1.67. *N*-(5-(4-fluorophenyl)-1,3,4-oxadiazol-2-yl)-3-(methoxy)-5-(trifluoromethyl)benzamide (**63**).

Prepared using general procedure A with **4D** (0.050 g, 0.28 mmol, 1.0 eq.), 3-methoxy-5-(trifluoromethyl) benzoyl chloride (0.080 g, 0.33 mmol, 1.2 eq.), and pyridine (2.0 mL) to produce **63** (0.032 g, 0.084 mmol, 30%) as a white solid. ^1H NMR (500 MHz, DMSO- d_6): δ 12.50 (s, 1H), 8.04-8.02 (m, 2H), 7.96 (s, 1H), 7.87 (s, 1H), 7.55 (s, 1H), 7.48 (t, $J = 8.7$ Hz, 2H), 3.94 (s, 3H). ^{13}C NMR (200 MHz, DMSO- d_6): δ 164.5

(d, $J = 250.0$ Hz), 160.7, 160.4, 160.3, 158.3, 135.3, 131.2 (q, $J = 32.0$ Hz), 129.2, 124.0 (q, $J = 270.0$ Hz), 120.4, 118.1, 117.4, 117.2 (d, $J = 22.0$ Hz), 115.5, 56.6. APCI-MS: m/z 382.2 $[M + H]^+$. HPLC retention time: 12.981 min. HPLC purity 100%.

5.1.68. *N*-(5-cyclohexyl-1,3,4-oxadiazol-2-yl)-3-(methyl)-5-(trifluoromethyl)benzamide (**64**).

Prepared using general procedure A with **4E** (0.036 g, 0.22 mmol, 1.0 eq.), 3-methyl-5-(trifluoromethyl)benzoyl chloride (0.058 g, 0.26 mmol, 1.2 eq.), and pyridine (2.0 mL) to produce **64** (0.022 g, 0.062 mmol, 29%). ^1H NMR (500 MHz, DMSO- d_6): δ 10.52 (s, 1H), 8.00 (broad s, 2H), 7.79 (s, 1H), 2.46 (s, 3H), 2.30 – 2.24 (m, 1H), 1.77– 1.72 (m, 4H), 1.65 – 1.63 (m, 1H), 1.43 – 1.36 (m, 2H), 1.27 – 1.17 (m, 4H). ^{13}C NMR (126 MHz, DMSO- d_6): δ 174.6, 164.2, 139.9, 133.4, 132.1, 129.3 (d, $J = 32.8$ Hz), 128.7, 124.0 (d, $J = 273.4$ Hz), 42.0, 29.1, 25.4, 25.2, 20.7. APCI-MS: m/z 354.2 $[M + H]^+$. HPLC retention time: 12.195 min. HPLC purity 98.6%.

5.1.69. *N*-(5-cyclohexyl-1,3,4-oxadiazol-2-yl)-4-(methyl)-3-(trifluoromethyl)benzamide (**65**).

Prepared using general procedure A with **4E** (0.030 g, 0.18 mmol, 1.0 eq.), 4-methyl-3-(trifluoromethyl)benzoyl chloride (0.048 g, 0.22 mmol, 1.2 eq.), and pyridine (2.0 mL) to produce **65** (0.016 g, 0.045 mmol, 25%) as a white solid. ^1H NMR (500 MHz, DMSO- d_6): δ 12.37 (s, 1H), 8.31 (s, 1H), 8.18 (d, $J = 8.1$ Hz, 1H), 7.60 (d, $J = 8.1$ Hz, 1H), 2.94-2.88 (m, 1H), 2.52 (s, 3H), 2.01 – 1.98 (m, 2H), 1.76-1.73 (m, 2H), 1.66 – 1.62 (m, 1H), 1.57-1.49 (m, 2H), 1.43-1.35 (m, 2H), 1.31-1.23 (m, 1H). APCI-MS: m/z 354.2 $[M + H]^+$. HPLC retention time: 13.367 min. HPLC purity 95.9%.

5.1.70. *N*-(5-cyclohexyl-1,3,4-oxadiazol-2-yl)-3-(methoxy)-5-(trifluoromethyl)benzamide (**66**).

Prepared using general procedure A with **4E** (0.050 g, 0.30 mmol, 1.0 eq.), 3-methoxy-5-(trifluoromethyl) benzoyl chloride (0.086 g, 0.36 mmol, 1.2 eq.), and pyridine (2.0 mL) to produce **66** (0.024 g, 0.065 mmol, 22%) as a white solid. ^1H NMR (500 MHz, DMSO- d_6): δ 12.52 (s, 1H), 7.92 (s, 1H), 7.84 (s, 1H), 7.50 (s, 1H), 3.35 (s, 3H), 2.94 – 2.90 (m, 1H), 2.04 – 1.98 (m, 2H), 1.77 – 1.73 (m, 2H), 1.66 – 1.62 (m, 1H), 1.57 – 1.49 (m, 2H), 1.43 – 1.35 (m, 2H), 1.31 – 1.23 (m, 1H). ^{13}C NMR (200 MHz, DMSO- d_6): δ 166.1, 160.3,

160.2, 159.3, 136.9, 131.0 (q, $J = 32.0$ Hz), 124.1 (q, $J = 272.0$ Hz), 118.0, 117.4, 115.0, 56.5, 34.6, 30.0, 25.7, 25.1. APCI-MS: m/z 370.3 $[M + H]^+$. HPLC retention time: 13.338 min. HPLC purity 98.6%.

5.2. Cell culture of HEK Cell lines

HEK293 cells stably expressing human AC1 or AC8 were maintained in Dulbecco's Modified Eagle's Medium (DMEM, Invitrogen, Carlsbad, CA) supplemented with 5% Fetal Clone I (HyClone GE Healthcare, Chicago, IL), 5% Bovine Calf Serum (Hyclone GE Healthcare, Chicago, IL), 1 % antibiotic-antimycotic (Gibco Thermo Fisher Scientific, Waltham, MA) and the selection antibiotic G418 (InvivoGen, San Diego, CA) at a concentration of 300 $\mu\text{g/mL}$ for the HEK-AC1 cell line or Puromycin (Sigma-Aldrich, St. Louis, MO) at a concentration of 200 $\mu\text{g/mL}$ for the HEK-AC8 cell line. Cells were grown in 15 cm dishes to an approximate 90% confluency and froze for cryopreservation as previously described [39].

5.3. cAMP accumulation assay

Cryopreserved HEK-AC1 and HEK-AC8 cells were quickly thawed and transferred into a 15 mL Falcon tube with pre-warmed Opti-MEM (Gibco Thermo Fisher Scientific, Waltham, MA). Cells were centrifuged at 150 x g for 5 minutes, supernatant was discarded, and cell pellet was resuspended in 1 mL of OptiMEM for cell counting. Cell suspension was adjusted to the desired cell density, cells were plated in a white opaque 384-well plate (Perkin Elmer, Waltham, MA) and incubated for 1 hour at 37°C with 5% CO₂. Cells were then treated with increasing concentrations of the compounds for 30 minutes at room temperature prior to the stimulation of AC activity with the calcium ionophore A23187 (Sigma-Aldrich, St. Louis, MO) at a final concentration of 3 μM and in the presence of 500 μM IBMX (Sigma-Aldrich, St. Louis, MO). Dose-response curves of 7 concentration points were generated for each compound with a 1:3 serial dilution starting at a concentration of 30 μM . After 1-hour incubation at room temperature with the stimulant, the Cisbio HTRF cAMP detection reagents (Cisbio, Bedford, MA), d2-labeled cAMP and anti-cAMP cryptate, were added to each well according to the manufacturer's instructions. Fluorescence reads at 620 nm and 665 nm emission wavelengths were measured with a Cytation 3 (Biotek, Winooski, VT) 1-hour after the addition of the detection reagents, and cAMP accumulation was determined for each well by interpolating the 620/665 signal ratios from a cAMP standard curve ran in parallel. The IC₅₀ values were calculated from the dose-response curves using Prism 7.0

(GraphPad Software, Inc. San Diego, CA) and the % inhibition at 30 μ M was calculated relative to the basal cAMP levels (100% inhibition) of each cell line.

5.4. AC1 homology modeling.

The sequence of human AC1 was obtained from the UNIPROT KB database (ID Q08828) [40]. A homology model of the cytoplasmic domains (residues 235 – 610 and 795 – 1119) were constructed based on two X-ray structures (PDB ID 1AZS and 3C16) [34, 41] using Schrodinger's homology modeling toolkit. The locations of the co-crystallized ligands in the template structures, i.e. ATP and forskolin, were transferred to the corresponding locations in the homology model. Cations and solvent molecules from the templates were not added to the homology model. The complex was finally optimized using Prime [42, 43].

5.5. Ligand-library and induced fit docking.

Sixty (60) compounds from the 1,3,4-oxadiazole series were prepared using Schrodinger's LigPrep toolkit and all possible tautomeric/protonation states of the ligands were generated. The series was docked into the homology model of AC1 using Schrodinger's Induced-Fit docking protocol [44-46] with the default configurations. Docking was performed into both binding sites, i.e. forskolin and ATP binding site, where the search volume was defined based on the centroid of the corresponding compound. For each 1,3,4-oxadiazole ligand, the top-20 poses were output.

All poses for all 60 ligands were clustered using Schrodinger's interactions clustering toolkit [47, 48]. First the fingerprints for the protein-ligand complexes were generated for any type of contact between the protein and the ligand. Then the similarity between the fingerprints were calculated using Tanimoto's metric and hierarchical clustering was performed. The optimal number of clusters were then computed by finding the cluster number with the least Kelley penalty value [49].

5.6. Cell viability assay.

For the cell viability assay, HEK-AC1 cells were plated and treated with the compounds and the AC stimulant as described above for the cAMP assays. The viability of the cells was determined at a single concentration of 30 μ M using the CellTiter-Glo Luminescent Cell Viability assay kit (Promega, Madison, WI).

After the pre-incubation for 30 minutes with the compound followed by 1-hour incubation with the AC stimulant, the CellTiter-Glo reagent was added under dim light to the wells according to the manufacturer's instructions. The final concentration of DMSO after the addition of the compound (30 μ M), the stimulant and the phosphodiesterase inhibitor (IBMX) was 0.19%. Luminescence was measured after 20 minutes incubation protected from light using a Synergy 4 (Biotek, Winooski, VT). Percentage cell viability was calculated relative to the luminescence counts of the vehicle (100% viable) and 2% Triton-X (0% viable) control wells.

5.7. Dose response analysis versus forskolin for AC1

HEK-AC Δ 3/6 cells, lacking AC3 and AC6 were transiently transfected with AC1 as previously described[29]. Cells were incubated with 3, 10, or 30 μ M forskolin in the presence of increasing concentrations of compound **6** or SQ22536 as indicated. Data were normalized to the matched forskolin response in the absence of drug and represent mean and S.E.M. of two- biological replicates completed in duplicate.

5.8. In vivo pain assay.

Mechanical sensitivity to tactile stimulation with von Frey filaments (Cat. #58011, Stoelting Co. Wood Dale, IL) was used to assess analgesia of the AC1 inhibitor as previously described[24]. In short, mice were confined to square plexiglass chambers and suspended on a wire grid platform without ability to see other test animals (Cat. #57816, Stoelting Co. Wood Dale, IL). Following habituation, a baseline response was measured using a modified up-and-down technique [50]. To induce a state of acute inflammation 8-week old C57BL/6 male mice (Envigo, Indianapolis, IN) were briefly anesthetized with isoflurane (5%) and while sedated received an intraplantar injection with 10 μ L emulsified CFA (1 mg/mL) in one of the hindpaws. The following day a new baseline was measured, and mice were intraperitoneally injected with the vehicle solubilized **61** (5 mg/kg; vehicle = 10% β -cyclodextrin in saline). Thirty minutes post drug injection mechanical sensitivity was recorded once more. The next day one final baseline was recorded. Mechanical sensitivity was normalized to baseline values. Mechanical sensitivity measurement statistical comparisons were carried out using Two-way repeated measure ANOVA with Bonferroni test in Prism 7.0 (Graphpad Software, Inc. San Diego, CA).

Upon arrival mice were grouped housed in single-grommet ventilated Plexiglas cages at ambient temperature (21°C) in a room maintained on a reversed 12-hour light/12-hour dark cycle (lights on at 700, lights off at 1900) in our animal facility certified by the Association for Assessment and Accreditation of Laboratory Animal Care. Food and water were provided *ad libitum*. The mice were given ~7 days to

acclimatize to the housing conditions before the start of the experiments. Mice were then habituated to the containment boxes for the von Frey assay. All animal procedures were preapproved by our Institutional Animal Care and Use Committee and were in accordance with the National Institutes of Health's Guide for the Care and Use of Laboratory Animals. Mice were not deprived of food or water at any time.

Conflicts of interest

The authors have declared no conflict of interest.

Acknowledgments

The want to acknowledge the assistance from Dr. Larissa Avramova and Dr. Lan Chen in the high-throughput screening. We also acknowledge Aaron Krabill, Lisha Ha, Jason Scott for assistance synthesizing selected analogs when necessary.

Funding

This work was supported by the National Institutes of Health [Grant R21/R33MH101673]; the Department of Medicinal Chemistry and Molecular Pharmacology Research Enhancement Award, the Purdue College of Pharmacy, Indiana CTSI Postdoctoral Challenge, and Purdue Chemical Genomics Facility.

References

- [1] D.M. Cooper, A.J. Crossthwaite, Higher-order organization and regulation of adenylyl cyclases, *Trends in pharmacological sciences*, 27 (2006) 426-431.
- [2] M. Zhuo, Cortical excitation and chronic pain, *Trends in neurosciences*, 31 (2008) 199-207.
- [3] E.R. Kandel, The molecular biology of memory storage: a dialogue between genes and synapses, *Science*, 294 (2001) 1030-1038.
- [4] H.S. Chan, D. McCarthy, J. Li, K. Palczewski, S. Yuan, Designing Safer Analgesics via μ -Opioid Receptor Pathways, *Trends in pharmacological sciences*, (2017).
- [5] R.K. Sunahara, R. Taussig, Isoforms of mammalian adenylyl cyclase: multiplicities of signaling, *Molecular interventions*, 2 (2002) 168.
- [6] R. Al-Hasani, M.R. Bruchas, Molecular mechanisms of opioid receptor-dependent signaling and behavior, *The Journal of the American Society of Anesthesiologists*, 115 (2011) 1363-1381.
- [7] L.M. Bohn, R.R. Gainetdinov, F.-T. Lin, R.J. Lefkowitz, M.G. Caron, μ -Opioid receptor desensitization by β -arrestin-2 determines morphine tolerance but not dependence, *Nature*, 408 (2000) 720.
- [8] K.M. Raehal, J.K. Walker, L.M. Bohn, Morphine side effects in β -arrestin 2 knockout mice, *Journal of Pharmacology and Experimental Therapeutics*, 314 (2005) 1195-1201.

- [9] K.M. Raehal, C.L. Schmid, C.E. Groer, L.M. Bohn, Functional selectivity at the μ -opioid receptor: implications for understanding opioid analgesia and tolerance, *Pharmacological reviews*, (2011) pr. 111.004598.
- [10] V.J. Watts, Selective Adenylyl Cyclase Type 1 Inhibitors as Potential Opioid Alternatives For Chronic Pain, *Neuropsychopharmacology*, 43 (2018) 215.
- [11] M. Zhuo, Targeting neuronal adenylyl cyclase for the treatment of chronic pain, *Drug discovery today*, 17 (2012) 573-582.
- [12] R. Sadana, C.W. Dessauer, Physiological roles for G protein-regulated adenylyl cyclase isoforms: insights from knockout and overexpression studies, *Neurosignals*, 17 (2009) 5-22.
- [13] A.C. Conti, J.W. Maas Jr, L.M. Muglia, B.A. Dave, S.K. Vogt, T.T. Tran, E.J. Rayhel, L.J. Muglia, Distinct regional and subcellular localization of adenylyl cyclases type 1 and 8 in mouse brain, *Neuroscience*, 146 (2007) 713-729.
- [14] C. Sanabra, G. Mengod, Neuroanatomical distribution and neurochemical characterization of cells expressing adenylyl cyclase isoforms in mouse and rat brain, *Journal of chemical neuroanatomy*, 41 (2011) 43-54.
- [15] M. Zhuo, A synaptic model for pain: long-term potentiation in the anterior cingulate cortex, *Molecules and cells*, 23 (2007) 259.
- [16] F. Wei, C.-S. Qiu, S.J. Kim, L. Muglia, J.W. Maas Jr, V.V. Pineda, H.-M. Xu, Z.-F. Chen, D.R. Storm, L.J. Muglia, Genetic elimination of behavioral sensitization in mice lacking calmodulin-stimulated adenylyl cyclases, *Neuron*, 36 (2002) 713-726.
- [17] G. Corder, S. Doolen, R.R. Donahue, M.K. Winter, B.L. Jutras, Y. He, X. Hu, J. Wieskopf, J. Mogil, D. Storm, Constitutive μ -opioid receptor activity leads to long-term endogenous analgesia and dependence, *Science*, 341 (2013) 1394-1399.
- [18] S.T. Wong, J. Athos, X.A. Figueroa, V.V. Pineda, M.L. Schaefer, C.C. Chavkin, L.J. Muglia, D.R. Storm, Calcium-stimulated adenylyl cyclase activity is critical for hippocampus-dependent long-term memory and late phase LTP, *Neuron*, 23 (1999) 787-798.
- [19] A.C. Emery, M.V. Eiden, L.E. Eiden, A new site and mechanism of action for the widely used adenylyl cyclase inhibitor SQ22, 536, *Molecular pharmacology*, (2012) mol. 112.081760.
- [20] R. Seifert, G.H. Lushington, T.-C. Mou, A. Gille, S.R. Sprang, Inhibitors of membranous adenylyl cyclases, *Trends in pharmacological sciences*, 33 (2012) 64-78.
- [21] K.I. Vadakkan, H. Wang, S.W. Ko, E. Zastepa, M.J. Petrovic, K.A. Sluka, M. Zhuo, Genetic reduction of chronic muscle pain in mice lacking calcium/calmodulin-stimulated adenylyl cyclases, *Molecular pain*, 2 (2006) 7.
- [22] H. Wang, H. Xu, L.-J. Wu, S.S. Kim, T. Chen, K. Koga, G. Descalzi, B. Gong, K.I. Vadakkan, X. Zhang, Identification of an adenylyl cyclase inhibitor for treating neuropathic and inflammatory pain, *Science translational medicine*, 3 (2011) 65ra63-65ra63.
- [23] C.S. Brand, H.J. Hocker, A.A. Gorfe, C.N. Cavasotto, C.W. Dessauer, Isoform selectivity of adenylyl cyclase inhibitors: characterization of known and novel compounds, *Journal of Pharmacology and Experimental Therapeutics*, 347 (2013) 265-275.
- [24] T.F. Brust, D. Alongkronrasmee, M. Soto-Velasquez, T.A. Baldwin, Z. Ye, M. Dai, C.W. Dessauer, R.M. van Rijn, V.J. Watts, Identification of a selective small-molecule inhibitor of type 1 adenylyl cyclase activity with analgesic properties, *Sci. Signal.*, 10 (2017) eaah5381.
- [25] J.B. Baell, G.A. Holloway, New substructure filters for removal of pan assay interference compounds (PAINS) from screening libraries and for their exclusion in bioassays, *Journal of medicinal chemistry*, 53 (2010) 2719-2740.
- [26] D. Lagorce, O. Sperandio, J.B. Baell, M.A. Miteva, B.O. Villoutreix, FAF-Drugs3: a web server for compound property calculation and chemical library design, *Nucleic acids research*, (2015) gkv353.
- [27] J.J. Irwin, D. Duan, H. Torosyan, A.K. Doak, K.T. Ziebart, T. Sterling, G. Tumanian, B.K. Shoichet, An Aggregation Advisor for Ligand Discovery, *Journal of medicinal chemistry*, 58 (2015) 7076-7087.

- [28] P. Niu, J. Kang, X. Tian, L. Song, H. Liu, J. Wu, W. Yu, J. Chang, Synthesis of 2-Amino-1, 3, 4-oxadiazoles and 2-Amino-1, 3, 4-thiadiazoles via Sequential Condensation and I₂-Mediated Oxidative C–O/C–S Bond Formation, *The Journal of organic chemistry*, 80 (2014) 1018-1024.
- [29] M. Soto-Velasquez, M.P. Hayes, A. Alpsoy, E.C. Dykhuizen, V.J. Watts, A Novel CRISPR/Cas9-Based Cellular Model to Explore Adenylyl Cyclase and cAMP Signaling, *Molecular pharmacology*, 94 (2018) 963-972.
- [30] P.D. Leeson, B. Springthorpe, The influence of drug-like concepts on decision-making in medicinal chemistry, *Nature Reviews Drug Discovery*, 6 (2007) 881-890.
- [31] M.D. Shultz, Setting expectations in molecular optimizations: strengths and limitations of commonly used composite parameters, *Bioorganic & medicinal chemistry letters*, 23 (2013) 5980-5991.
- [32] M.D. Shultz, The thermodynamic basis for the use of lipophilic efficiency (LipE) in enthalpic optimizations, *Bioorganic & medicinal chemistry letters*, 23 (2013) 5992-6000.
- [33] C.W. Dessauer, V.J. Watts, R.S. Ostrom, M. Conti, S. Dove, R. Seifert, International union of basic and clinical pharmacology. Cl. Structures and small molecule modulators of mammalian adenylyl cyclases, *Pharmacological reviews*, 69 (2017) 93-139.
- [34] J.J. Tesmer, R.K. Sunahara, A.G. Gilman, S.R. Sprang, Crystal structure of the catalytic domains of adenylyl cyclase in a complex with Gs α · GTP γ S, *Science*, 278 (1997) 1907-1916.
- [35] N. Rana, J.M. Conley, M. Soto-Velasquez, F. León, S.J. Cutler, V.J. Watts, M.A. Lill, Molecular Modeling Evaluation of the Enantiomers of a Novel Adenylyl Cyclase 2 Inhibitor, *Journal of chemical information and modeling*, 57 (2017) 322-334.
- [36] C.W. Murray, D.A. Erlanson, A.L. Hopkins, G.r.M. Keserü, P.D. Leeson, D.C. Rees, C.H. Reynolds, N.J. Richmond, Validity of ligand efficiency metrics, *ACS medicinal chemistry letters*, 5 (2014) 616-618.
- [37] W.-b. Kang, Q. Yang, Y.-y. Guo, L. Wang, D.-s. Wang, Q. Cheng, X.-m. Li, J. Tang, J.-n. Zhao, G. Liu, Analgesic effects of adenylyl cyclase inhibitor NB001 on bone cancer pain in a mouse model, *Molecular pain*, 12 (2016) 1744806916652409.
- [38] Z. Tian, D.-s. Wang, X.-s. Wang, J. Tian, J. Han, Y.-y. Guo, B. Feng, N. Zhang, M.-g. Zhao, S.-b. Liu, Analgesic effects of NB001 on mouse models of arthralgia, *Molecular brain*, 8 (2015) 60.
- [39] J.M. Conley, T.F. Brust, R. Xu, K.D. Burris, V.J. Watts, Drug-induced sensitization of adenylyl cyclase: assay streamlining and miniaturization for small molecule and siRNA screening applications, *Journal of visualized experiments: JoVE*, (2014).
- [40] R. Apweiler, A. Bairoch, C.H. Wu, W.C. Barker, B. Boeckmann, S. Ferro, E. Gasteiger, H. Huang, R. Lopez, M. Magrane, UniProt: the universal protein knowledgebase, *Nucleic acids research*, 32 (2004) D115-D119.
- [41] T.-C. Mou, N. Masada, D.M. Cooper, S.R. Sprang, Structural basis for inhibition of mammalian adenylyl cyclase by calcium, *Biochemistry*, 48 (2009) 3387-3397.
- [42] M.P. Jacobson, R.A. Friesner, Z. Xiang, B. Honig, On the role of the crystal environment in determining protein side-chain conformations, *Journal of molecular biology*, 320 (2002) 597-608.
- [43] M.P. Jacobson, D.L. Pincus, C.S. Rapp, T.J. Day, B. Honig, D.E. Shaw, R.A. Friesner, A hierarchical approach to all-atom protein loop prediction, *Proteins: Structure, Function, and Bioinformatics*, 55 (2004) 351-367.
- [44] R. Farid, T. Day, R.A. Friesner, R.A. Pearlstein, New insights about HERG blockade obtained from protein modeling, potential energy mapping, and docking studies, *Bioorganic & medicinal chemistry*, 14 (2006) 3160-3173.
- [45] W. Sherman, H.S. Beard, R. Farid, Use of an induced fit receptor structure in virtual screening, *Chemical biology & drug design*, 67 (2006) 83-84.
- [46] W. Sherman, T. Day, M.P. Jacobson, R.A. Friesner, R. Farid, Novel procedure for modeling ligand/receptor induced fit effects, *Journal of medicinal chemistry*, 49 (2006) 534-553.
- [47] J. Duan, S.L. Dixon, J.F. Lowrie, W. Sherman, Analysis and comparison of 2D fingerprints: insights into database screening performance using eight fingerprint methods, *Journal of Molecular Graphics and Modelling*, 29 (2010) 157-170.

- [48] M. Sastry, J.F. Lowrie, S.L. Dixon, W. Sherman, Large-scale systematic analysis of 2D fingerprint methods and parameters to improve virtual screening enrichments, *Journal of chemical information and modeling*, 50 (2010) 771-784.
- [49] L.A. Kelley, S.P. Gardner, M.J. Sutcliffe, An automated approach for clustering an ensemble of NMR-derived protein structures into conformationally related subfamilies, *Protein Engineering, Design and Selection*, 9 (1996) 1063-1065.
- [50] D. Alongkronrusmee, T. Chiang, R.M. van Rijn, Involvement of delta opioid receptors in alcohol withdrawal-induced mechanical allodynia in male C57BL/6 mice, *Drug and alcohol dependence*, 167 (2016) 190-198.

Highlights for manuscript reference number EJMECH-D-18-02224 – “Optimization of a 1,3,4-oxadiazole series for inhibition of Ca^{2+} /calmodulin-stimulated activity of adenylyl cyclases 1 and 8 for the treatment of chronic pain”

- The 1,3,4-oxadiazole scaffold is identified as a novel small molecule with cellular inhibitory activity against AC1- and AC8-mediated cAMP production.
- 65 analogs were synthesized and tested for activity in HEK-AC1 and HEK-AC8 expressing cell lines for their ability to inhibit Ca^{2+} /calmodulin-mediated cAMP production.
- A selected analog was shown to provide a modest analgesic effect in an *in vivo* mouse model for inflammatory pain.
- The data in the study further suggests inhibition of AC1-mediated cAMP production is a viable therapeutic approach to treat chronic pain.